III. Distance Ladder

I. Aretxaga

Ene-Jun 2012

Distance Ladder: solar system ($\sim 10^{-6}$ pc)

Radars

Direct measurement of the distance to Venus and other objects in a near-Earth orbit with **radar**:

Measure the time it takes for a radar signal to arrive at Venus, bounce off and reflect back to Earth, where it is detected.

$$2d = c \times t$$
$$d = c \times t/2$$

Example: during closest approach of Venus in 1961, powerful radars were installed on the Mk 1 telescope and also at the 70m Goldstone dish in New Mexico. Pulsed radar signals were transmitted towards Venus reaching it 2 min later. Reflected radio pulses were detected 4 minutes later. Time of the pulse can be measured accurately and the distance to Venus calculated (41.4 million km).

Distance Ladder: solar system (~10^{-6} pc)

Triangulation

From the measured distance Earth-Venus, the distance of Earth from the Sun (1 AU) was determined:

$$d_{\text{Earth-Sun}} = d_{\text{Earth-Venus}} / \cos\theta$$

$$d_{\text{Earth-Sun}} = 149{,}597{,}892 \text{ km} = 1 \text{ AU}$$

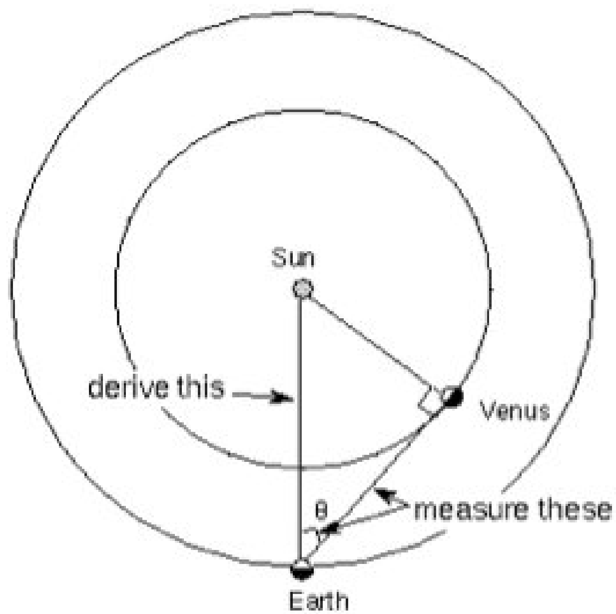

Measuring the angle θ between Venus and the Sun and the distance between Earth and Venus enables us to find the distance between the Earth and the Sun using trigonometry.

Distance Ladder: solar system (~10^{-6} pc)

Orbits

Kepler's 3rd law allows determination of distance by measuring the orbital period:

"The ratio of the squares of the periods of any two planets is equal to the ratio of the cubes of their average distances from the sun."

period^2 / radius^3 = constant

$$T_{Earth}^2 / R_{Earth}^3 = \text{constant} = T_{Mars}^2 / R_{Mars}^3$$

$$T_{Earth}^2 / T_{Mars}^2 = R_{Earth}^3 / R_{Mars}^3$$

$$R_{Mars} = R_{Earth} \times (T_{Mars} / T_{Earth})^{2/3}$$

$$R_{Mars} = R_{Earth} \times (687 \text{ days} / 365.256 \text{ days})^{2/3}$$

$$R_{Mars} = 1.52 \times R_{Earth}$$

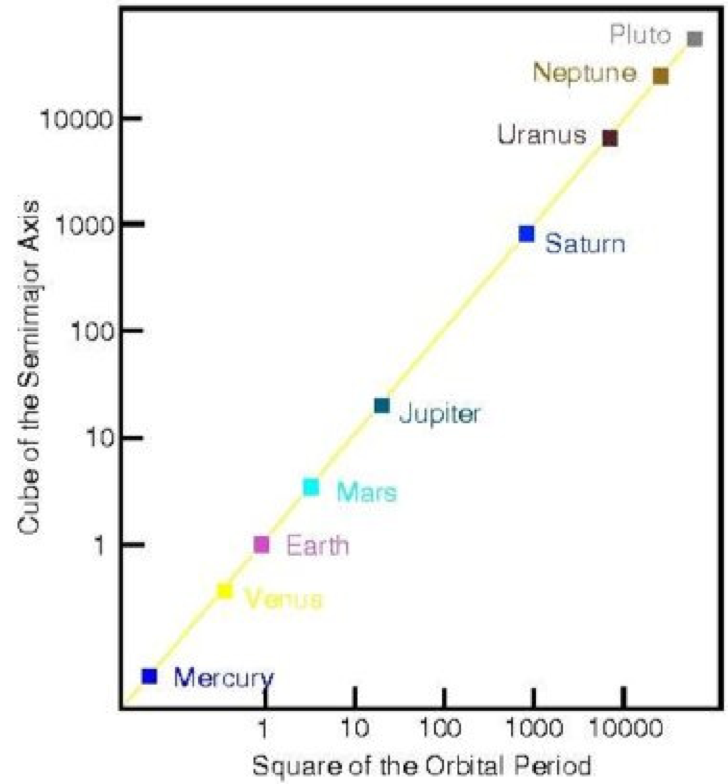

Distance Ladder: nearby stars (~50 pc)

Trigonometric Parallaxes

$$\tan \pi = 1 \text{ AU} / d$$
$$d \text{ [pc]} = 1 / \tan \pi \text{ [radians]}$$
for small angles π: $\tan \pi \approx \pi$
or
Distance [pc] = 1 / Parallax [arc seconds]

Nearest star (α Cen) has a parallax of 0.76'' $\Rightarrow$ distance is 1/0.76 = 1.3 pc

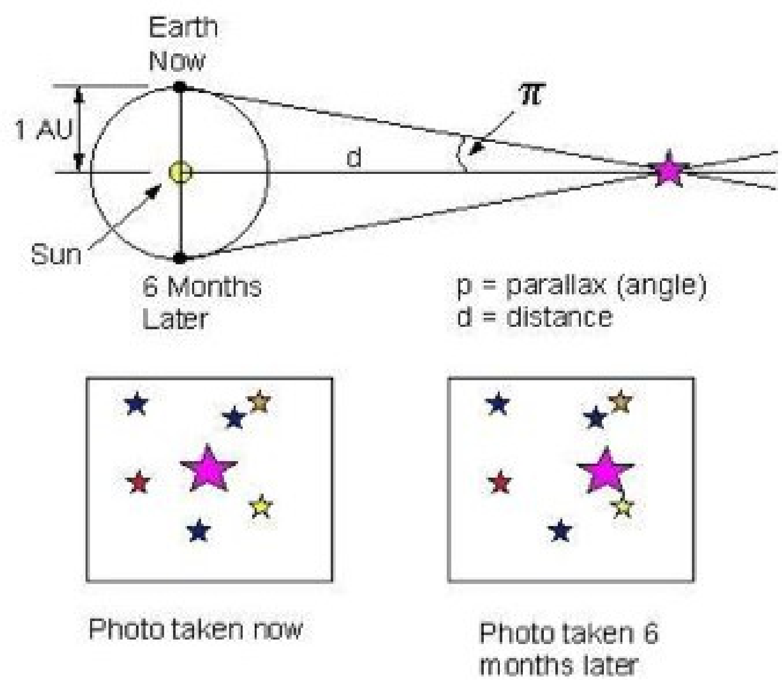

Distance Ladder: nearby stars (~1kpc)

Next mission Gaia (ESA, 2013) to 1Mpc

Limitations: until 1990, could only detect parallaxes out to 50 pc.

Hipparcos satellite (ESA) (1990–93):

Designed to measure parallaxes of stars with unprecedented accuracy.

Can detect parallaxes out to 1 kpc.

Used to map out the locations of nearby stars with an accuracy of 1–2 milli-arcsec (size of a golf ball viewed from the other side of the Atlantic Ocean)

'*Tycho Star Catalogue*' contains more than one million stars – ~120000 with astrometric parameters

Distance Ladder: Hyades (moving cluster)

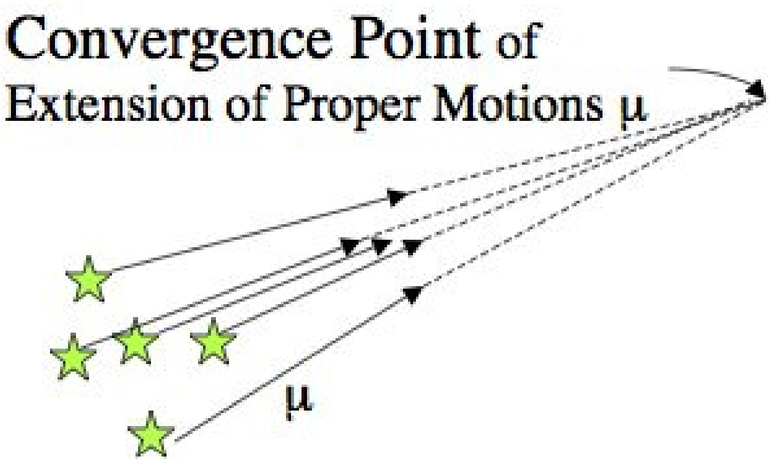

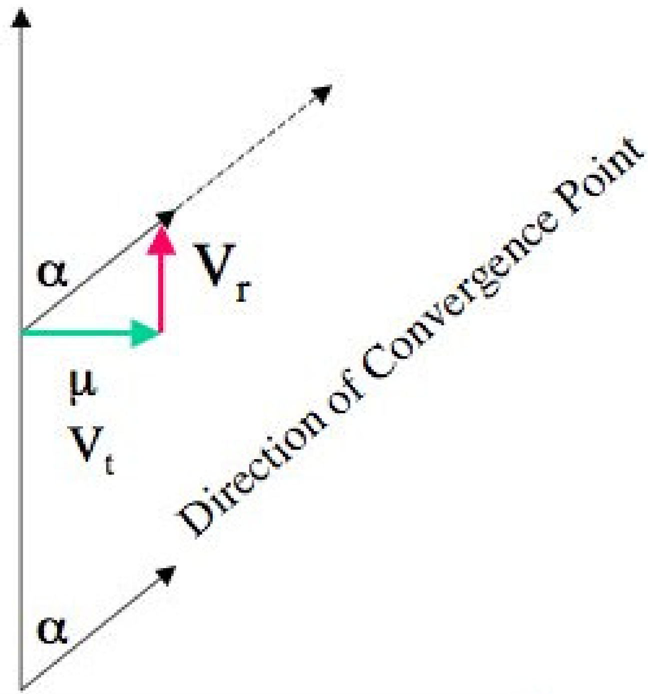

1) μ = proper motion (arcsec per year)
 $= V_t$ (km/s) / 4.74xD(pc)

V_t= transverse velocity D=distance

2) Velocities in radial direction V_r (km/s)

3) Angle to convergence point α

Tan α $= V_t/V_r$ but

$$\text{Distance(pc)} = \frac{V_T}{4.74\,\mu} \quad \text{so}$$

$$= \frac{V_R(km/s)Tan\alpha}{4.74\,\mu(arc\sec/yr)}$$

Distance Ladder: Statistical Parallax (~300pc)

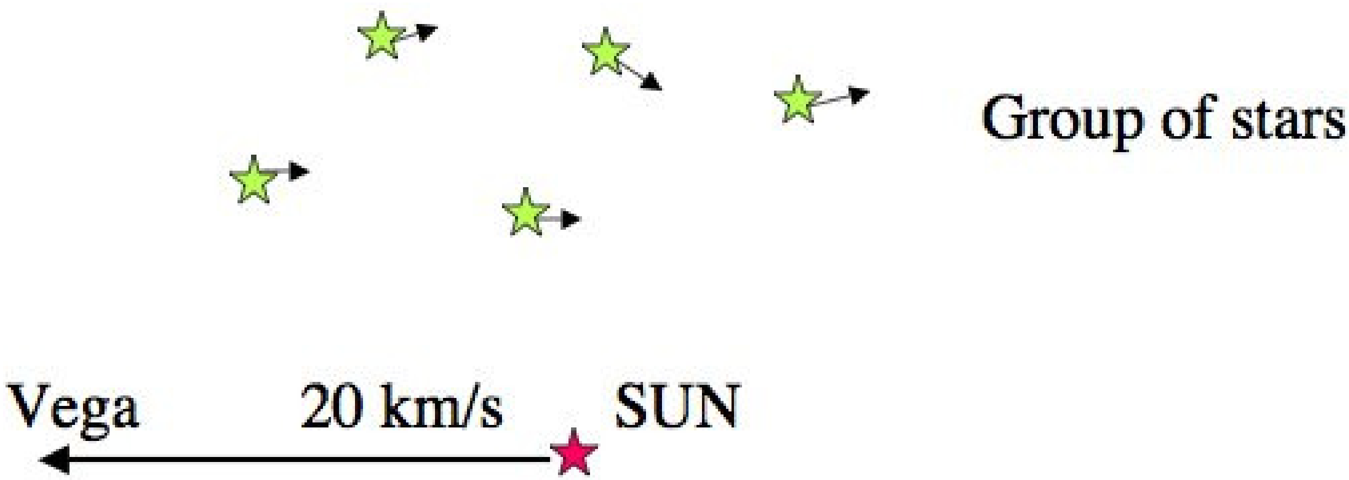

Sun travels ~ 4 A.U. per year so after 20 years, the baseline for parallax is ~ 80 A.U. ~ 40x longer than normal parallax.

Proper motions (μ) combined with radial velocities (Vr) to get *AVERAGE* distances of a group of stars.

$$D \propto \frac{\sigma(v_r)}{\sigma(\mu)}$$

Distance Ladder

Primary Indicators:

- can be measured in nearby galaxies
- small dispersion around a well defined mean
- can be calibrated through geometrical means

e.g. cepheids, novas, RR Lyrae, BA supergiants, eclipsing binaries, …

Secondary, tertiary, … indicators:

- are calibrated through primary, secondary… indicators

e.g. Type Ia supernovae, Tully-Fisher, D_n-σ, brightest stars, planetary nebulae, …

Primary Indicators: Cepheids (~20 Mpc)

Cepheid stars are long-period variables (~1-100 days) and they display a tight luminosity-period linear relationship (better than 10% precision), which is weakly dependent on metallicity.

$$\boxed{M_V = -2.80 \log P_{\mathrm{d}} - (1.43 \pm 0.1)}$$ (Feast & Catchpole 1997)

$$\boxed{\delta(m-M)_0 = -0.24 \pm 0.16}$$ (Kennicut et al. 1998) Metal rich brighter

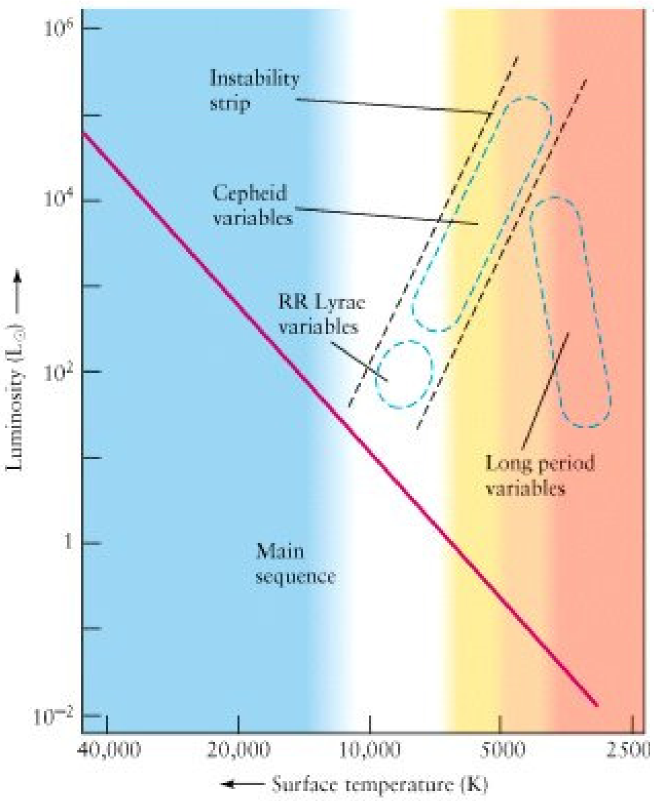

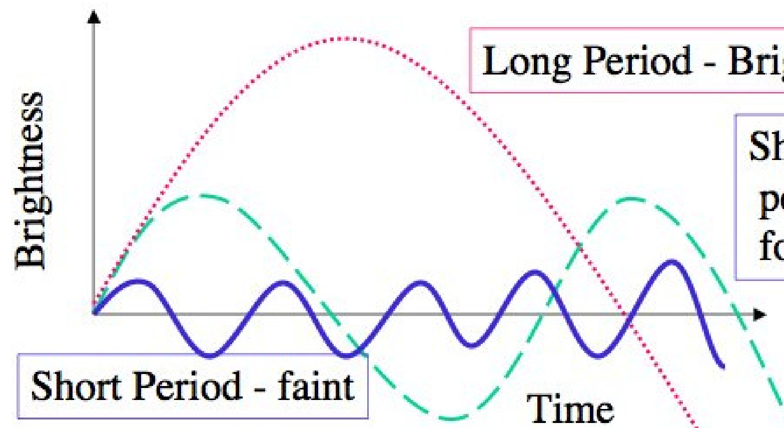

Shows relation of period and brightness for Cepheid variables.

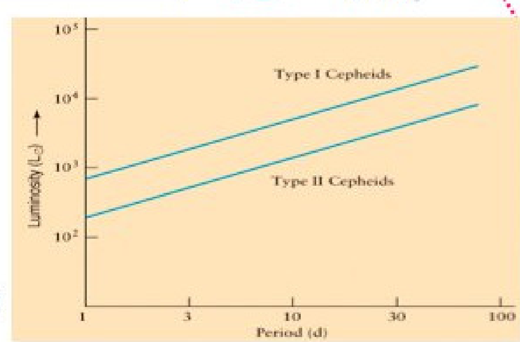

Note there are two Cepheid relations, with Type I in plane of Milky Way vs Type II in globular clusters.

Primary Indicators: Cepheids (~20 Mpc)

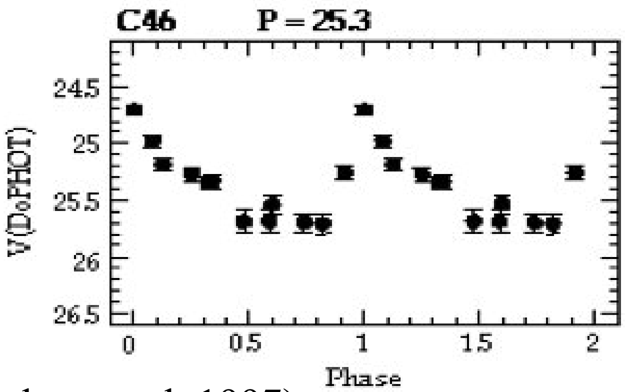

(Kelson et al. 1997)

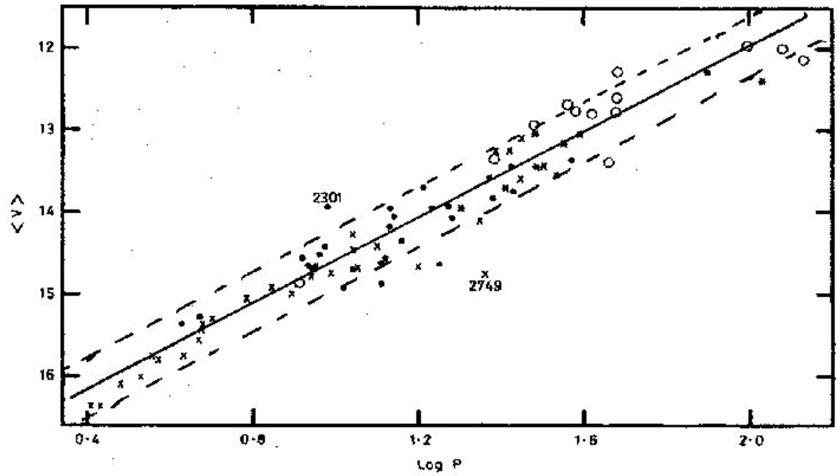

(Madore & Freedman 2001)

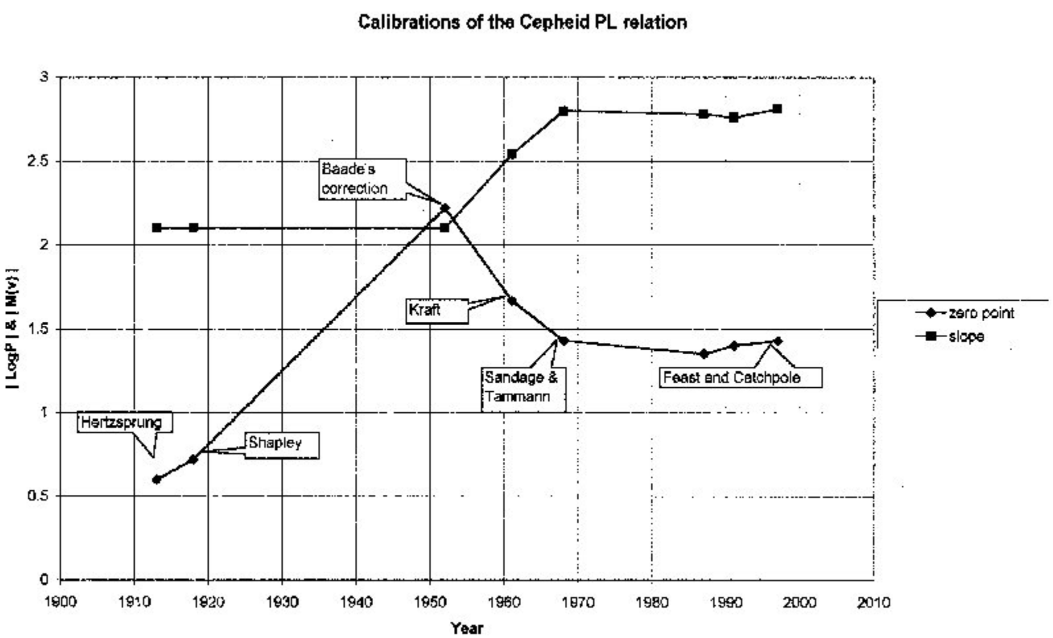

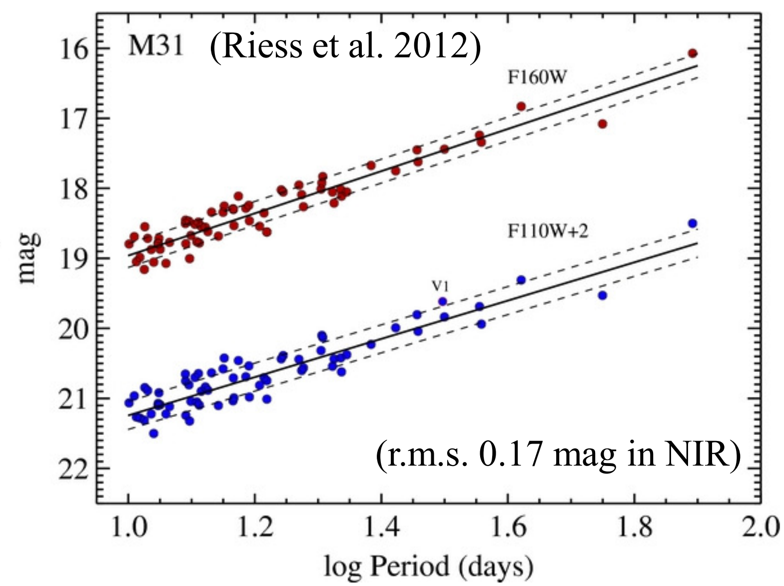

(Allen 2001: http://www.institute-of-brilliant-failures.com/index.htm)

Primary Indicators: Cepheids (~20 Mpc)

H_0 Key Project

- What do we do with all of these distances?
- H_0 Key Project – started in 1990, final results 2001!
  - Observe Cepheids in ~18 spiral galaxies to test the universality of the Cepheid P-L relation and greatly improve calibration of other distance indicators which generally rest on one or two local group galaxies
  - Their Cepheid P-L relation zeropoint is tied directly to the distance to the LMC (largest source of error in current estimate of H_0!)
  - Combining different estimators, they find H_0=72 +/- 3 (random) +/- 7 (systematic) km/s/Mpc !
  - But note that it's not over yet as some people disagree with their adopted value for the distance to the LMC …
  - … and other methods give different answers!

Other primary Indicators: main sequence (~10 kpc)

Main Sequence Fitting

Most stars are located on the Main Sequence in the HR Diagram:

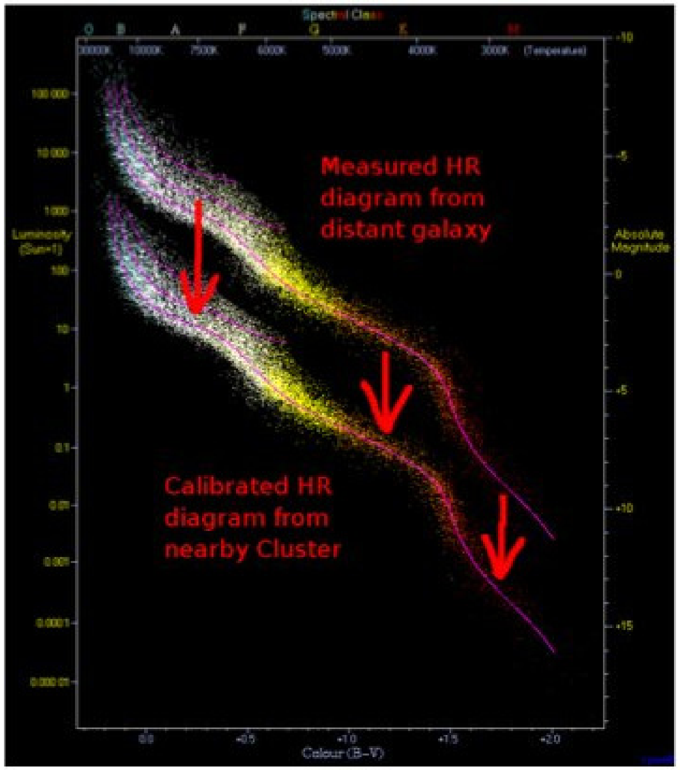

$$m - M = -5 + 5 \log_{10} d$$

Other primary Indicators:

Eclipsing binaries: Uses Kepler's 3rd law, Stefan-Boltzmann relationship and assumes a M/L.

Novas: relationship between maximum Luminosity and decay time

RR Lyrae: constant magnitude and color.

BA Supergiant Stars: based on the Barbier & Chalonge classification method, which measures the Balmer break.

Secondary Indicators: type Ia SNe (~4Gpc)

Not really a standard candle, but a candle that can calibrated
Advantages: - bright
- small dispersion (<0.3 mag)
- small corrections for absorption
- they occur in all Hubble types

Barbon Ciatti & Rosino 197

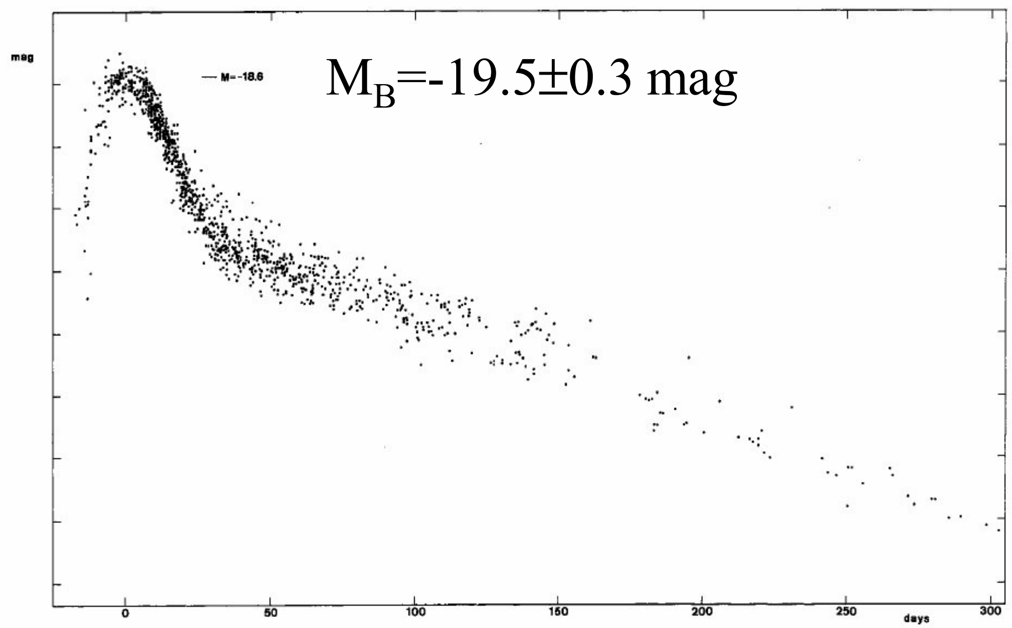

Fig. 1. Average blue light curve, obtained by the fitting (as explained in the text) of the observations of 38 type I supernovae (see Table 1). One magnitude intervals are marked on the ordinates

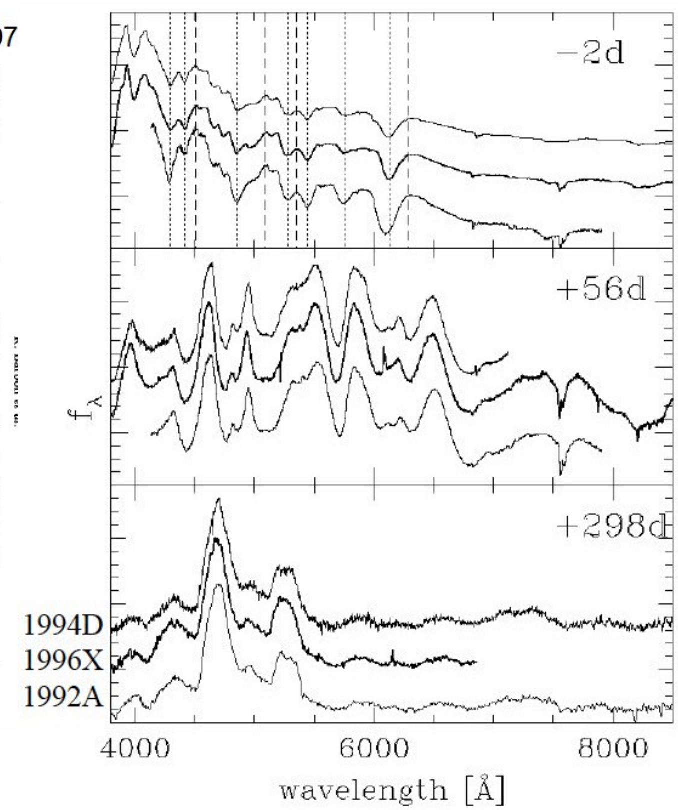

SNe: taxonomy

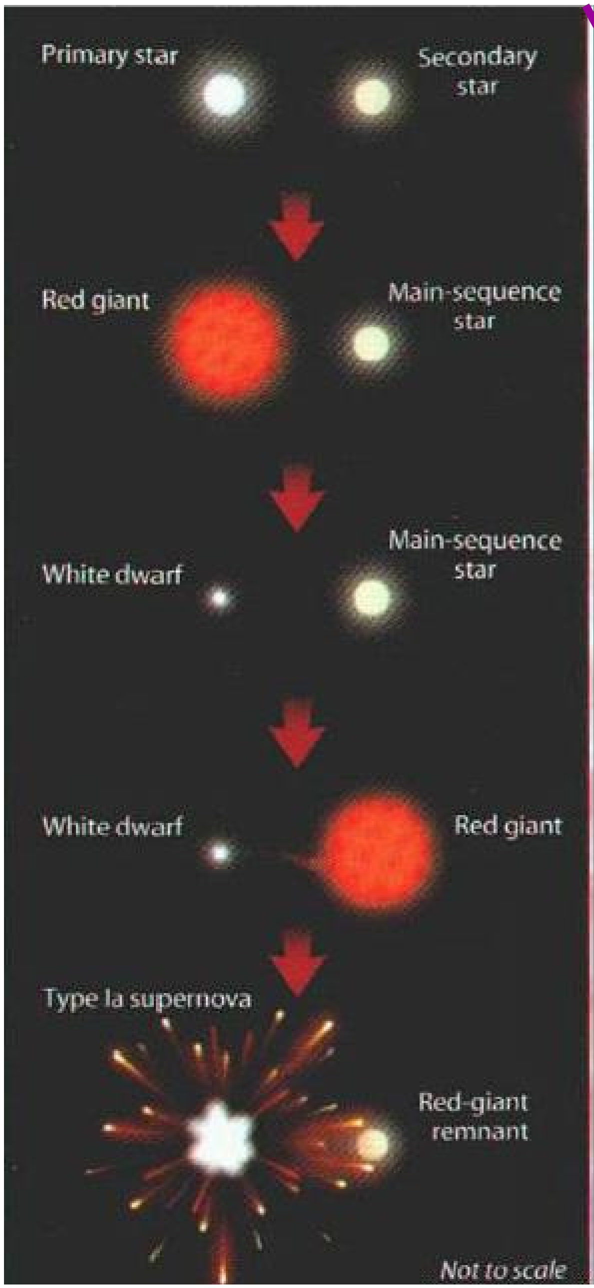

Early Spectra:

No Hydrogen / Hydrogen

SN I
Si/ No Si

SN II
~3 mos. spectra
He dominant/H dominant

SN Ia
1985A
1989B

He poor/He rich

SN Ic
1983I
1983V

SN Ib
1983N
1984L

SN IIb
1993J
1987K

"Normal" SNII

Light Curve decay after maximum:

Believed to originate from ***deflagration*** or ***detonation*** of an ***accreting white dwarf***.

Core Col
Outer Lay
by winds
or binary
Ib: H mar
Ic: H & H

Theory

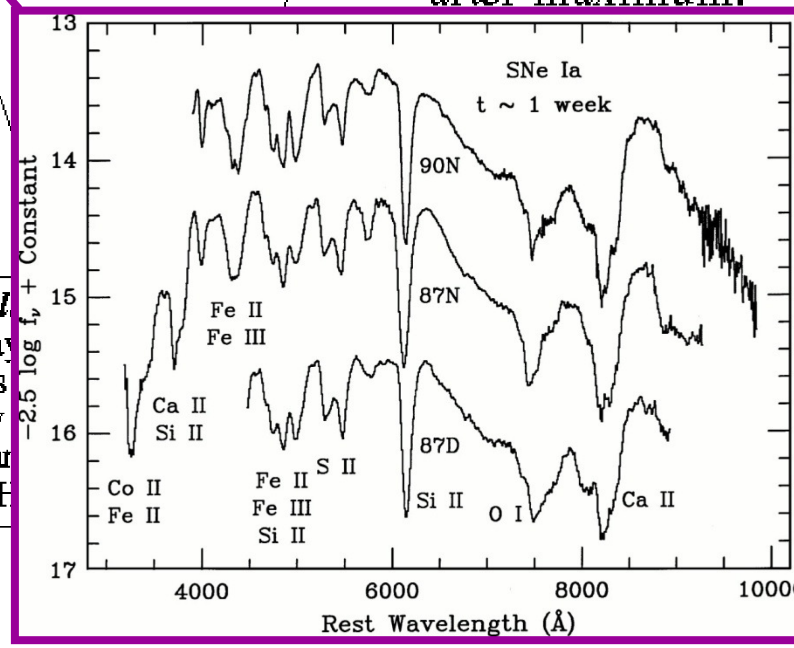

(Filippenko 1997)

SNe: taxonomy

Early Spectra:

No Hydrogen

SN I
Si/ No Si

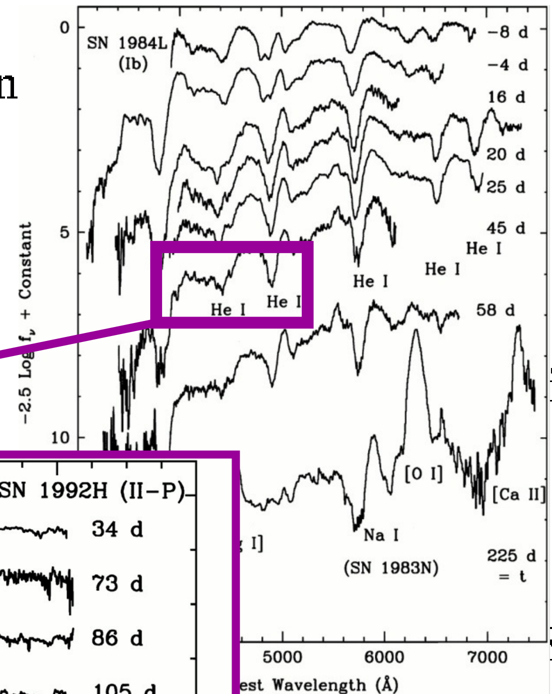

inant

SNII

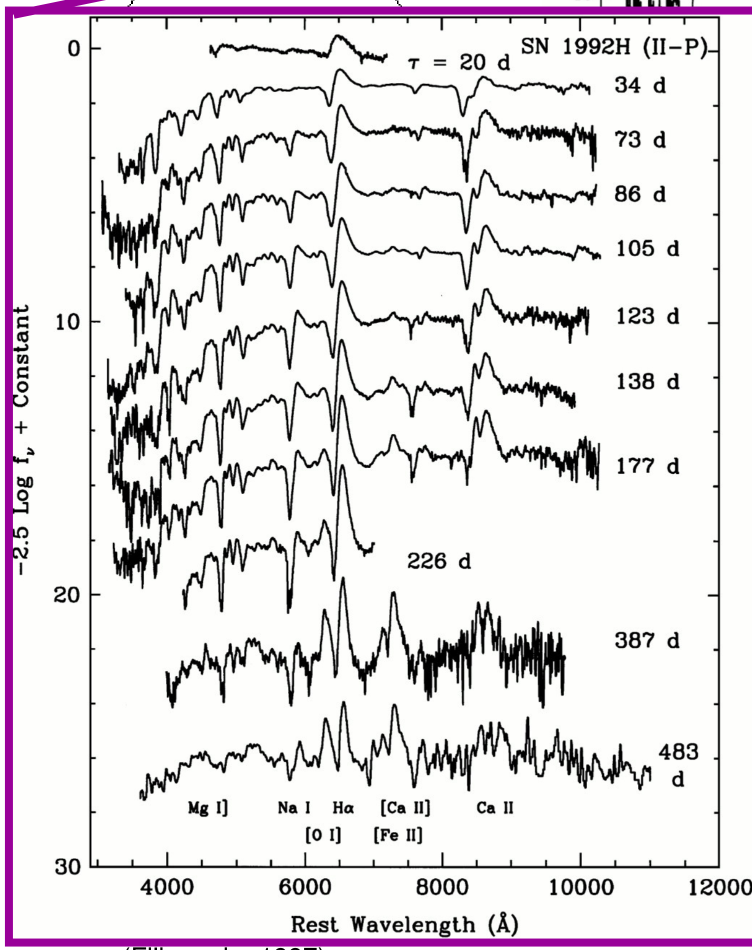

(Filippenko 1997)

ng

Light Curve decay
after maximum:
Linear / Plateau

SN IIL	SN IIP
1980K 1979C	1987A 1988A 1969L

Core Collapse of
a massive progenitor
with plenty of H .

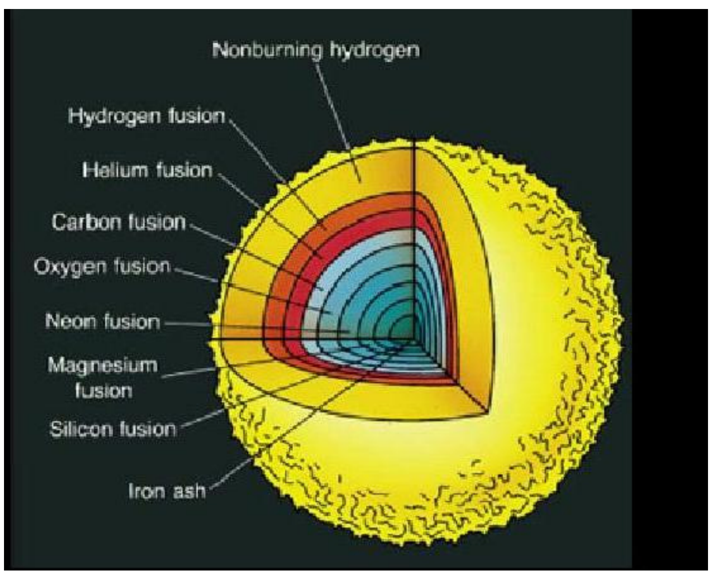

SNe: taxonomy

Early Spectra: No Hydrogen / Hydrogen

SN I
Si/ No Si

SN II
~3 mos. spectra
He dominant/H dominant

SN Ia
1985A
1989B

He poor/He rich

SN Ic
983I
983V

SN Ib
1983N
1984L

SN IIb
1993J
1987K

"Normal" SNII

Light Curve decay after maximum:
Linear / Plateau

originate
ation or
of an
hite dwarf.

Core collapse.
Most (NOT all)
H is removed during
evolution by
tidal stripping.

SN IIL
1980K
1979C

SN IIP
1987A
1988A
1969L

Core Collapse.
Outer Layers stripped
by winds (*Wolf-Rayet Stars*)
or binary interactions
Ib: H mantle removed
Ic: H & He removed

Core Collapse of
a massive progenitor
with plenty of H .

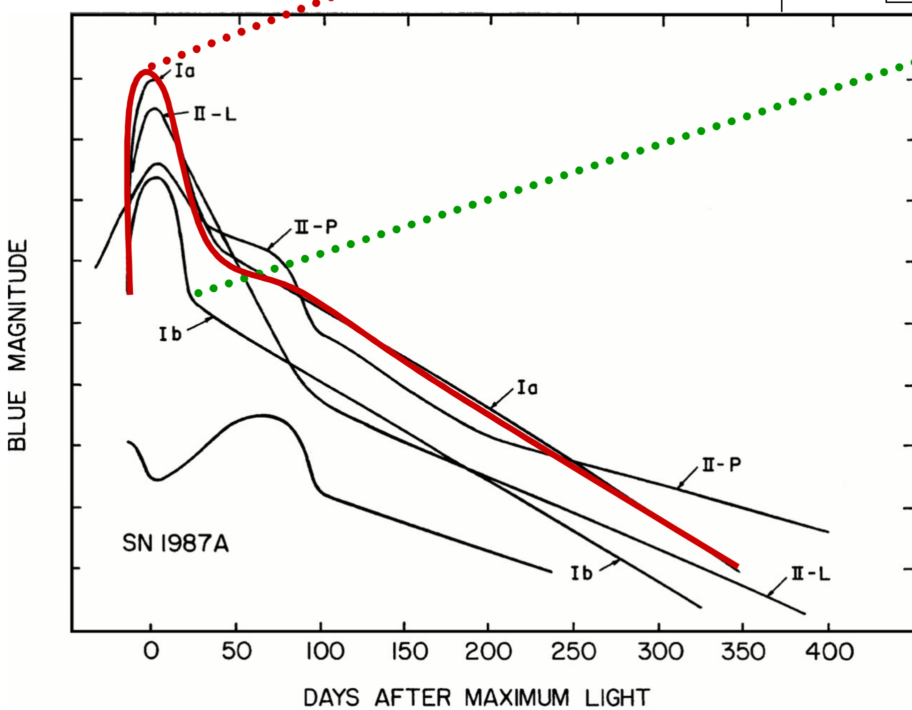

Secondary Indicators: type Ia SNe (~4Gpc)

Not really a standard candle, but a candle that can be calibrated

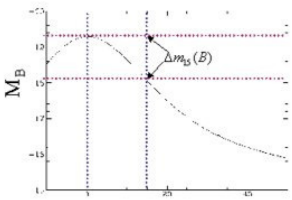

galactic only galactic + host E(B-V)<0.1

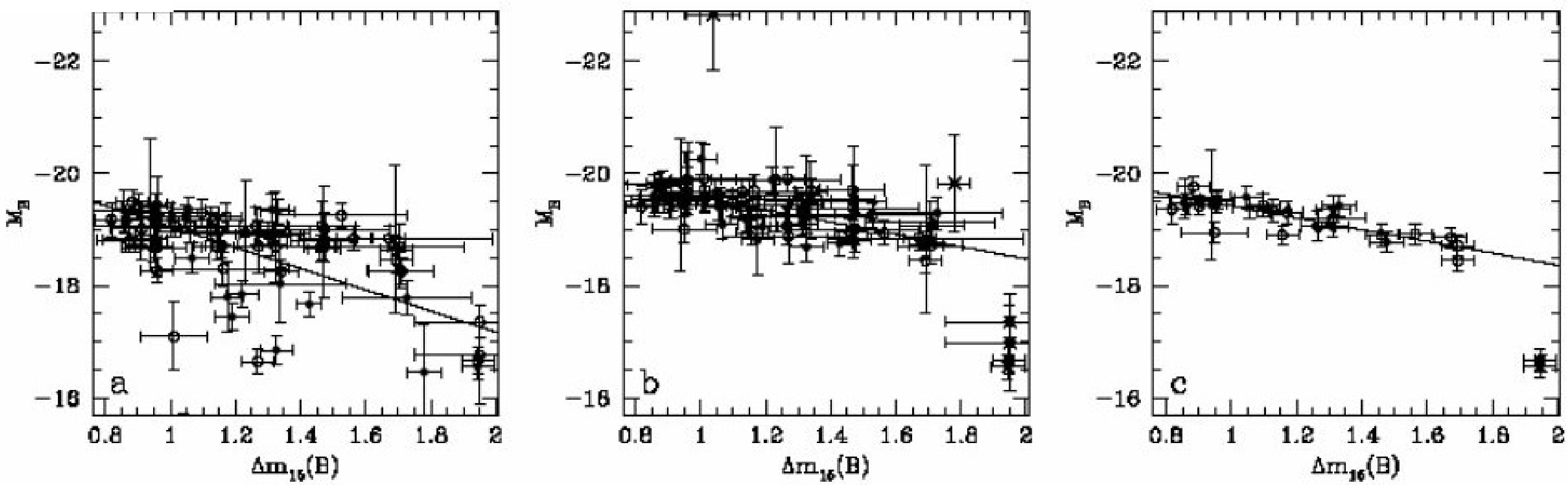

Figure 5. M_B versus $\Delta m_{15}(B)$ relation; filled circles indicate objects whose distances are given by Tully's catalogue, open symbols are objects whose distances are calculated from their recession velocity. The linear fit is weighted in both axes (Press 1992). **a**: Only galactic reddening correction applied. Number of objects used for the linear fit n=73, dispersion $\sigma = 0.83$. **b**: Both Galactic and host galaxy reddening corrections applied. The outliers, marked with a cross, are (from left to right, from top to bottom): SN 1996ai, which is characterized by high and not well known reddening; SN 1986G, another highly reddened event; SN 1992K, 1999da, 1998de, 1991bg, which are peculiar sub-luminous events. The latters seem to form a separate class and do not fit the linear relation defined by all others. n=67, $\sigma = 0.31$. **c**: as the previous case but selecting only SNe with $E(B-V) < 0.1$ and small errors (< 0.2) in $\Delta m_{15}(B)$. n=26, $\sigma = 0.20$. $R_B = 3.5$.

(Hamuy et al. 1996)

Secondary Indicators: type Ia SNe (~4Gpc)

Not really a standard candle, but a candle that can be calibrated

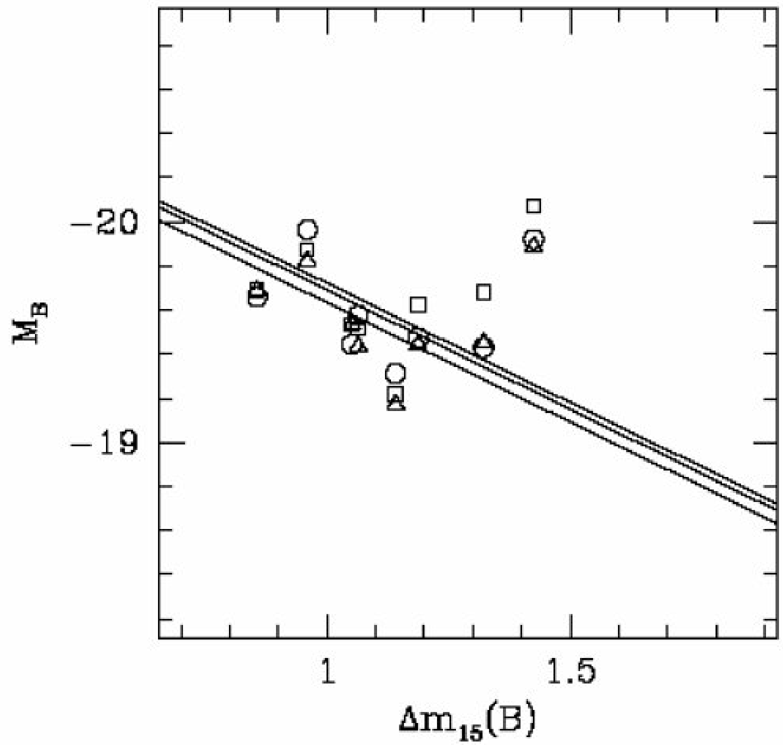

Figure 8. M_B versus $\Delta m_{15}(B)$ for 8 of the 9 SNe calibrated by Cepheids (SN 1960F has been excluded because colour information required to estimate the host galaxy extinction is not available). Circles: Distance modulus μ from Freedman et al. 2001; triangles: μ corrected assuming $\Delta Y/\Delta Z = 2.5$; square: μ corrected assuming $\Delta Y/\Delta Z = 3.5$. Solid lines are the best fits obtained with a fixed slope minimizing the deviation of the three sets of Cepheids calibrated SNe. The slope (1.082) is the same as in Fig. 5c.

Secondary Indicators: type Ia SNe (~4Gpc)

$$M_B = a\,(\Delta m_{15} - 1.1) + b$$

Table 1. Parameters of the M_B=a$(\Delta m_{15}(B) - 1.1) + b$ relation. From top to bottom: values obtained for case **b**, **c** (as in §2.3). From left to right: number of objects used for the correlation; R_B adopted; slope (error); zero point derived from three different assumptions on the metallicity PL relation (error); dispersion.

n	R_B	a	b				σ
			KP	$\Delta Y/\Delta Z = 2.5$	$\Delta Y/\Delta Z = 3.5$		
67	4.315	1.102 (0.147)	-19.613	-19.523	-19.582	(0.037)	0.31
67	3.5	1.092 (0.124)	-19.460	-19.399	-19.472	(0.031)	0.28
26	3.5	1.061 (0.154)	-19.455	-19.403	-19.476	(0.044)	0.20

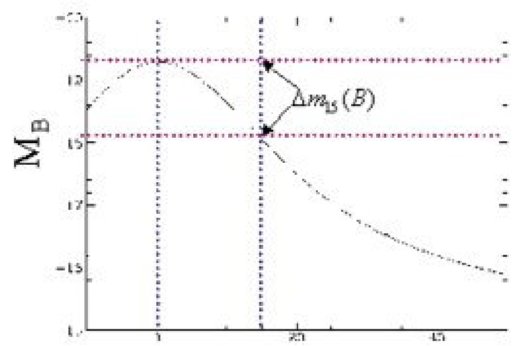

Hamuy et al. 1996, b=-19.258-+0.048

Secondary Indicators: high-z SNe (~4Gpc)

Two teams doing high-z SN searches to measure cosmological parameters:

- Supernova Cosmology Project (http://panisse.lbl.gov/ , P.I. Saul Perlmutter)
- High-z SN Search (http://cfa-www.harvard.edu/supernova//HighZ.html, P.I. Brian Schmidt)

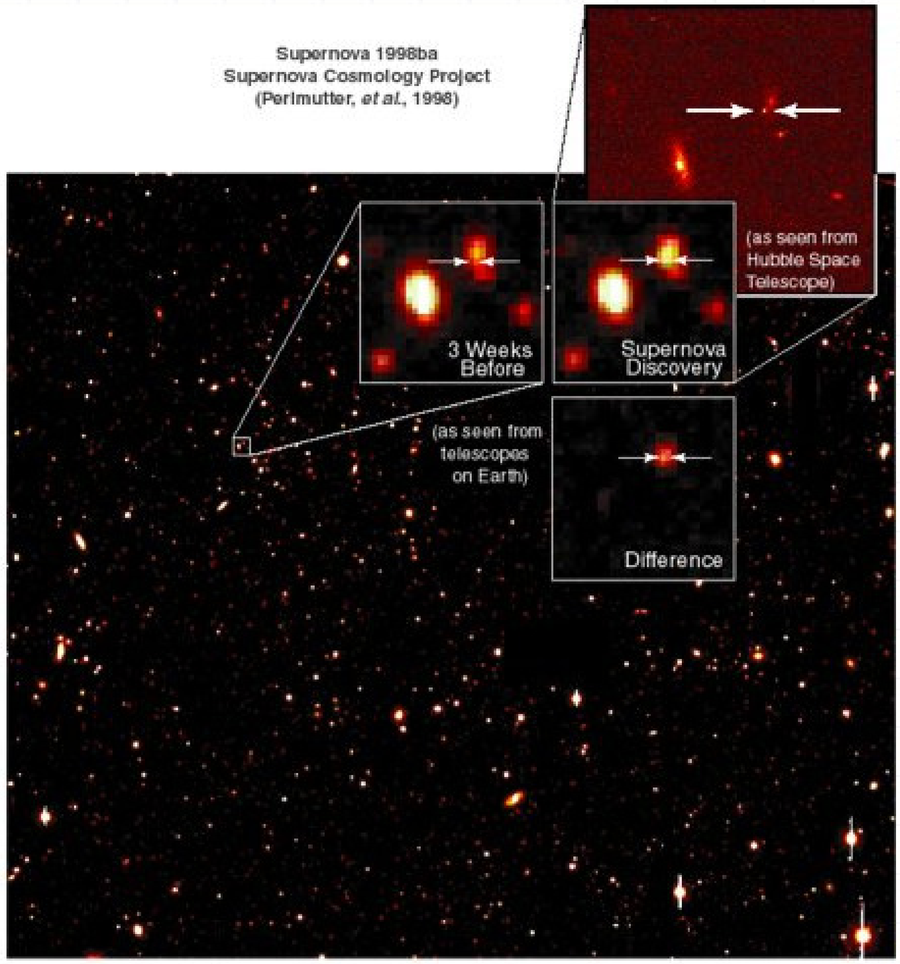

Secondary Indicators: high-z SNe (~4Gpc)

Two teams doing high-z SN searches to measure cosmological parameters:

- Supernova Cosmology Project (http://panisse.lbl.gov/ , P.I. Saul Perlmutter)
- High-z SN Search (http://cfa-www.harvard.edu/supernova//HighZ.html, P.I. Brian Schmidt)

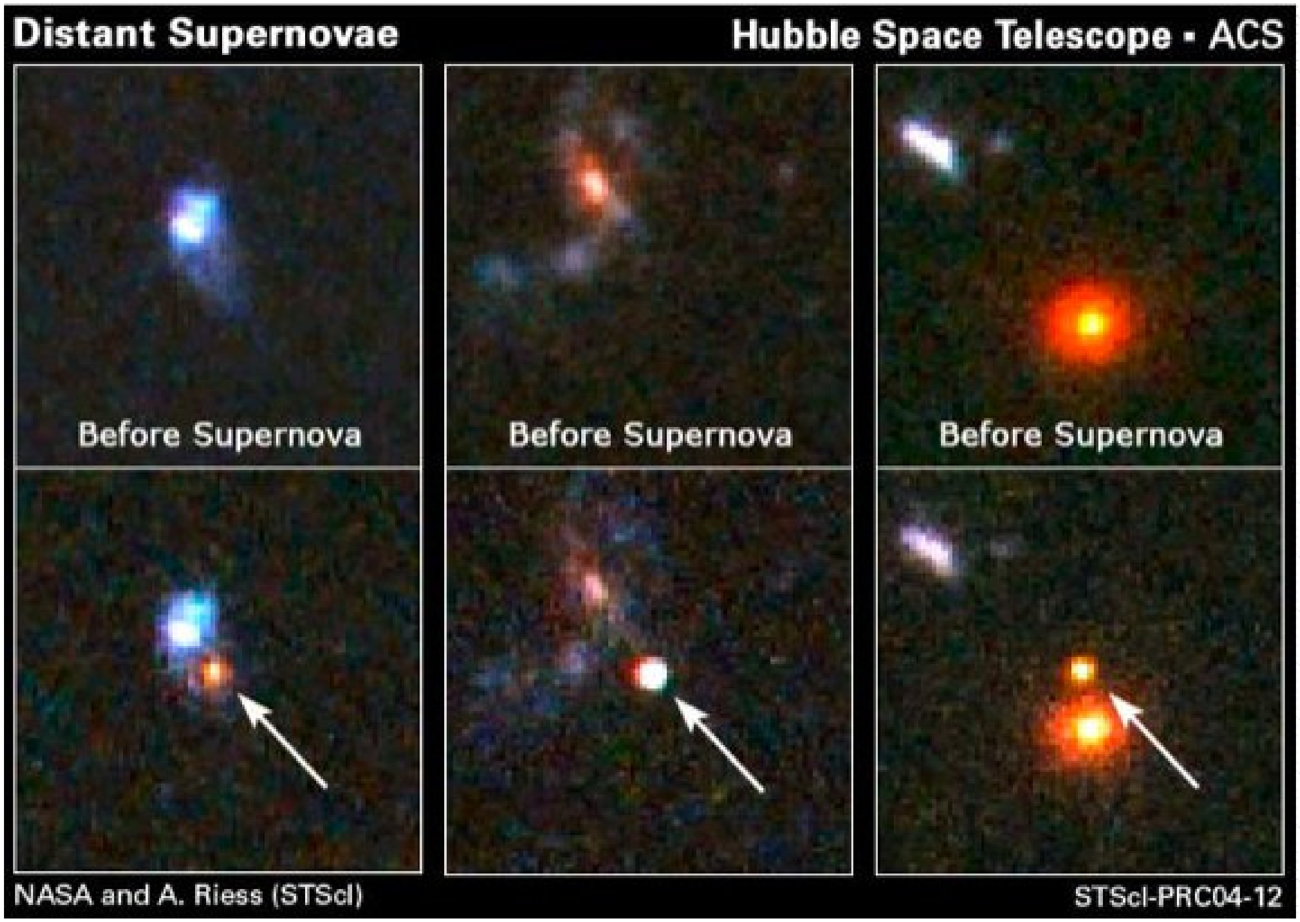

Secondary Indicators: high-z SNe (~4Gpc)

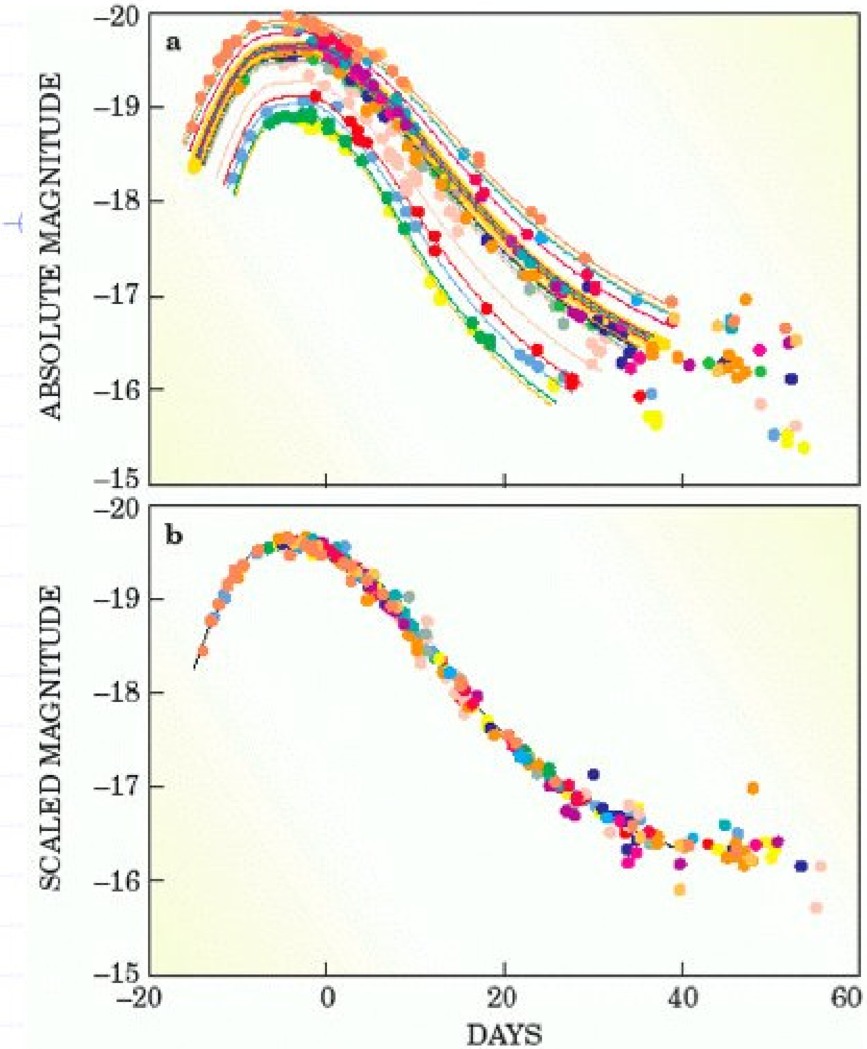

New methods to relate shape and luminosity and standardize luminosity at maximum:

SN Cosmo Project: Stretch method
(Perlmutter et al. 1997)
High-z SN project: Multi-colour light-shape fitting method
(Riess et al. 1996)

Secondary Indicators: high-z SNe (~4Gpc)

Examples of light-curves by High-z SN Search Project (Garnavich et al. 1995)

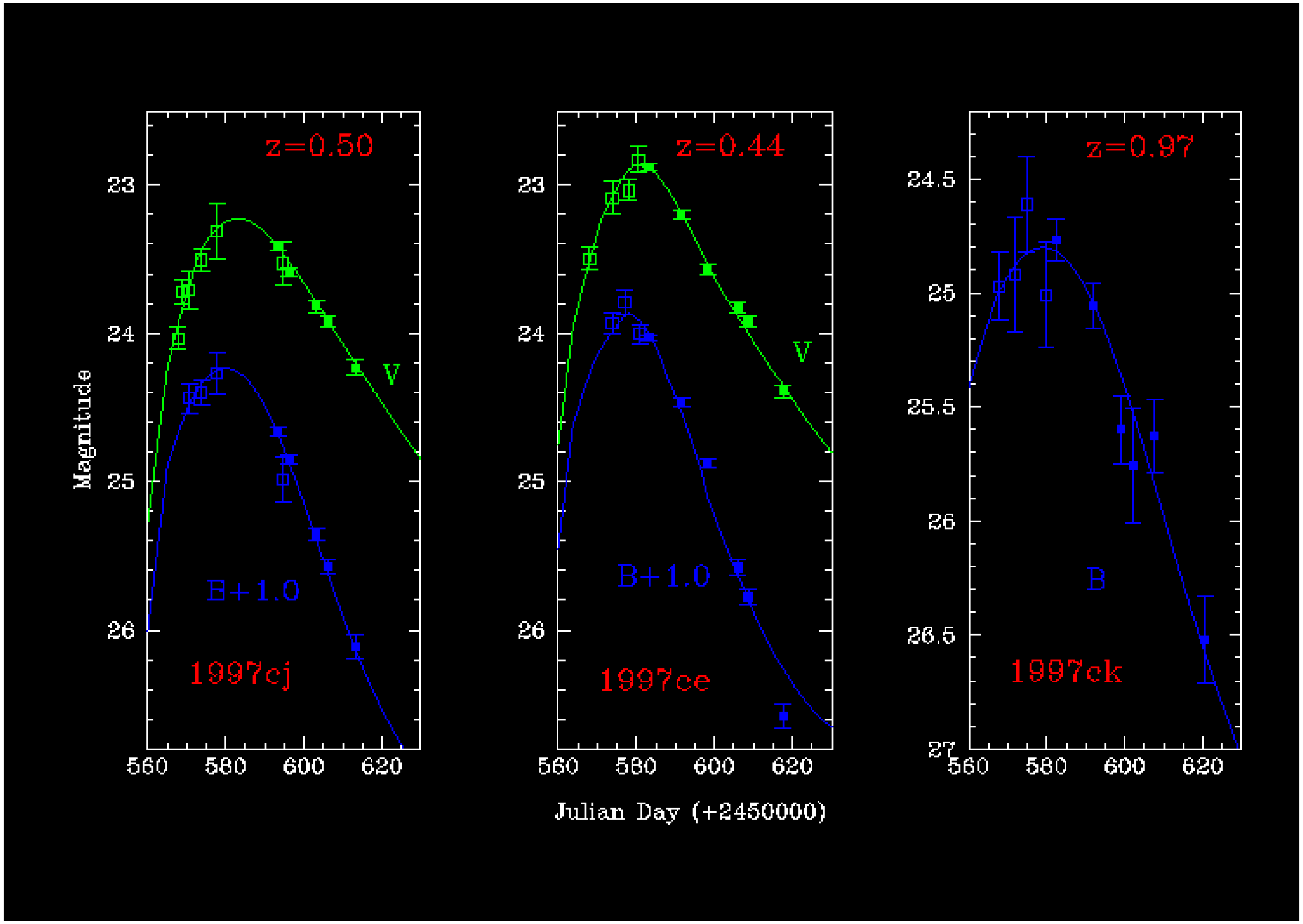

Secondary Indicators: Tully-Fisher (~100Mpc)

The Tully-Fisher relates the velocity width and luminosity of spiral galaxies, or in other words: it gives a correlation for spiral galaxies between their luminosity and how fast they are rotating.

The circular velocity in galaxies scales as:

$$M \propto V_c^2 R$$

The mass-to-light ratio (M/L) can be parameterized as:

$$M = L * (M/L)$$

Assuming the surface brightness (SB) of galaxies is the same for spiral galaxies (*SB* = luminosity per unit area) we can write *L* in terms of *R* ans *SB*:

$$SB = L/area = L/R^2; \quad L = SB * R^2 \quad \rightarrow L \propto R^2$$

We can rewrite this as

$$L * (M/L) \propto V_c^2 * L^{1/2}$$

We further assume that *M/L* is constant:

$$L^{1/2} \propto V_c^2 \rightarrow L \propto V_c^4$$

Now we convert to magnitudes and keeping in mind that $M = -2.5 \log L$ *gives*

$$M \propto -10 Log V_c$$

This equation states that the mass of a galaxy is proportional to the circular velocity of the spiral arms. *M/L* = const.

Bottom Line: if you measure the velocity dispersion of a galaxy, you can infer the mass and luminosity and distance.

Secondary Indicators: Tully-Fisher (~100Mpc)

- Typically work in I-band (compromise between less scatter and detector size & response)
- Can be used at large distances since we're using luminous spirals
- Disadvantages – extinction due to dust is a problem (work in IR if possible), scatter in relation means it is best for determining the distances to groups & clusters of galaxies instead of to individual galaxies, inclination corrections are uncertain
- We're not sure why it works, why is the product of the mass to light ratio times the surface brightness a constant (remember this is what is required for $L \sim V^4$)

Secondary Indicators: Tully-Fisher (~100Mpc)

Tully-Fisher at various wavelengths

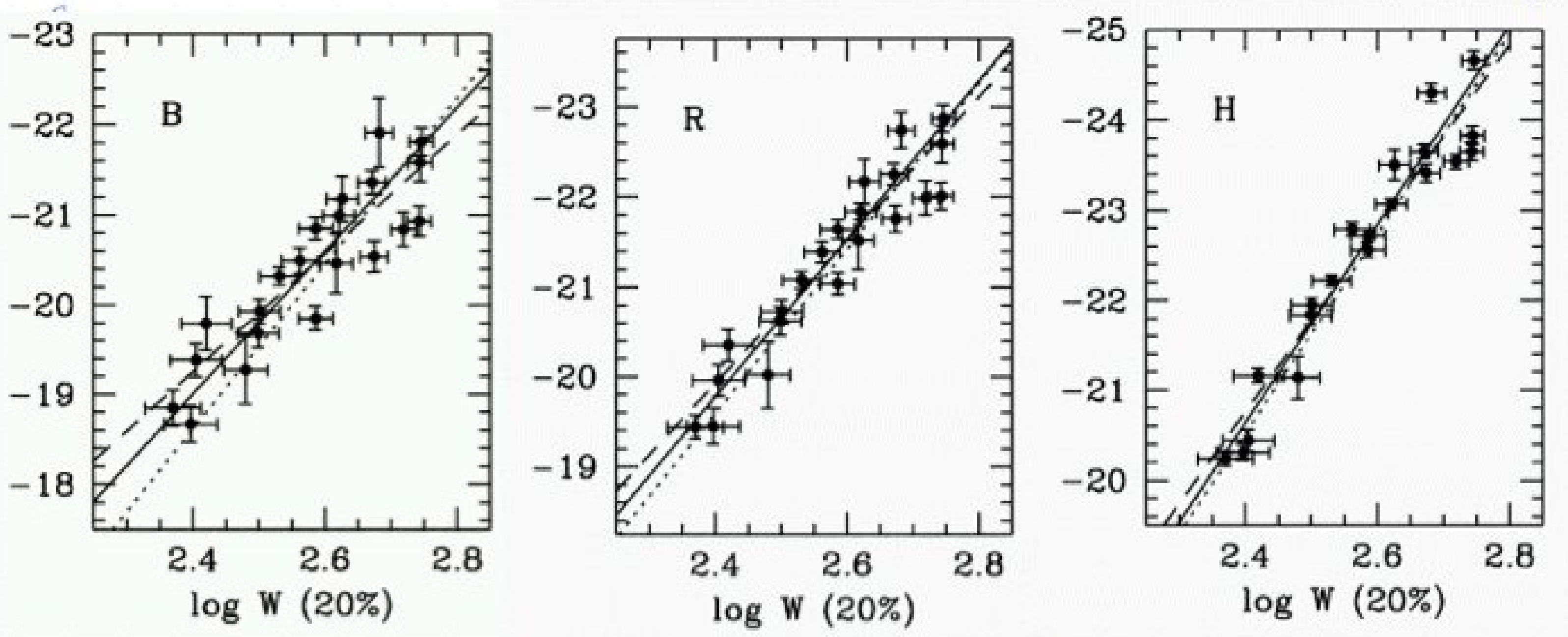

α= 3.2
Scatter=0.25 mag

α= 3.5
Scatter=0.25 mag

α= 4.4
Scatter=0.19 mag

Note, M = a log W + b

Secondary Indicators: Tully-Fisher (~100Mpc)

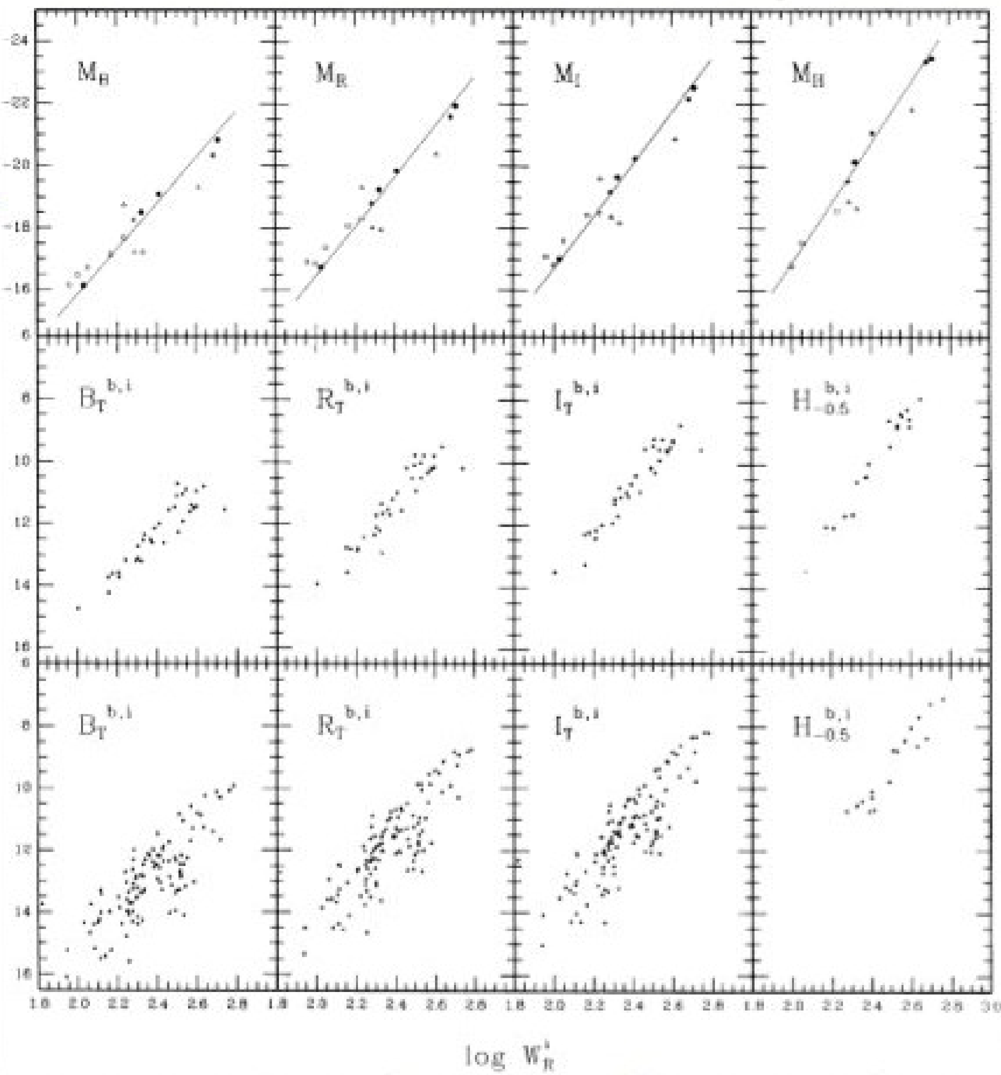

Local Group

Ursa Major

Virgo

TF at various distances, from Jacoby et al 1992

Secondary Indicators: "extended" Tully-Fisher (~4Gpc)

THE STELLAR MASS TULLY-FISHER RELATION TO $Z = 1.2$ FROM AEGIS

SUSAN A. KASSIN[1], BENJAMIN J. WEINER[2], S. M. FABER[1], DAVID C. KOO[1], JENNIFER M. LOTZ[3], JÜRG DIEMAND[1,4], JUSTIN J. HARKER[1], KEVIN BUNDY[5], A. J. METEVIER[1], ANDREW C. PHILLIPS[1], MICHAEL C. COOPER[6], DARREN J. CROTON[5], NICHOLAS KONIDARIS[1], KAI G. NOESKE[1], & C. N. A. WILLMER[2,7]

Accepted for Publication in the ApJL

(ApJ 2008)

ABSTRACT

We combine newly measured rotation velocities, velocity dispersions, and stellar masses to construct stellar mass Tully-Fisher relations (M_*TFRs) for 544 galaxies with strong emission lines at $0.1 < z < 1.2$ from the All Wavelength Extended Groth Strip International Survey (AEGIS) and the Deep Extragalactic Evolutionary Probe 2 Survey (DEEP2). The conventional M_*TFR using only rotation velocity (V_{rot}) shows large scatter (~ 1.5 dex in velocity). The scatter and residuals are correlated with morphology in the sense that disturbed, compact, and major merger galaxies have lower velocities for their masses. We construct an M_*TFR using the kinematic estimator $S_{0.5}$ which is defined as $\sqrt{0.5V_{rot}^2 + \sigma_g^2}$ and accounts for disordered or non-circular motions through the gas velocity dispersion (σ_g). The new M_*TFR, termed $S_{0.5}/M_*$TFR, is remarkably tight over $0.1 < z < 1.2$ with no detectable evolution of its intercept or slope with redshift. The average best fit relation has 0.47 dex scatter in stellar mass, corresponding to ~ 1.2 'magnitudes,' assuming a constant mass-to-light ratio. Interestingly, the $S_{0.5}/M_*$TFR is consistent with the absorption-line based stellar mass Faber-Jackson relation for nearby elliptical galaxies in terms of slope and intercept, which might suggest a physical connection between the two relations.

$$S_{0.5} = \sqrt{0.5v_{rot}^2 + \sigma_{gas}^2}$$

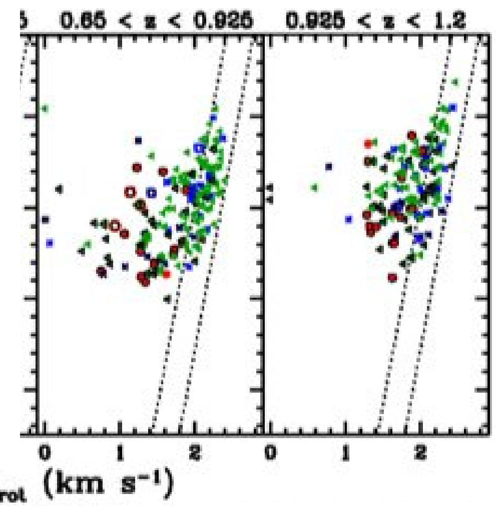

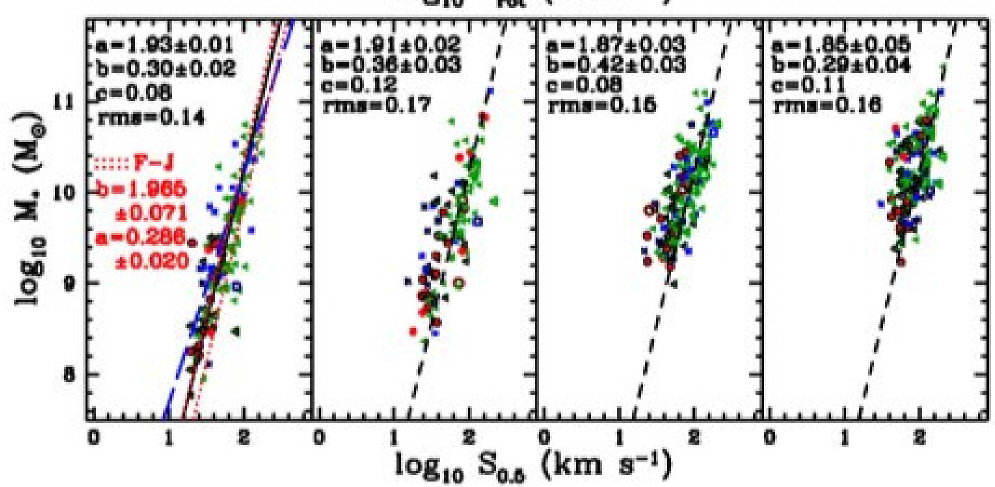

Secondary Indicators: D_n-σ (~1Gpc)

E galaxies have a fundamental plane that links their surface brightness, luminosity and velocity dispersion: $L \propto I_0^x \sigma^y$ with x~ –0.7, y~0.3 (Dressler et al. 1987, Djorgovski & Davis 1987).

This relationship can be understood if E gal are self-gravitating systems with roughly constant M/L ratios.

Virial Theorem $\sigma^2 \propto M / r_0$

$M/L \propto M^a$

de Vaucouleurs profile $\Rightarrow L \propto I_0 r_0^2$

$$\longrightarrow \quad L^{1+a} \propto \sigma^{4-4a} I_0^{a-1}$$

If we measure the diameter of an E gal within which the mean surface brightness takes some reference value $D_n \propto r_0^{\alpha} I_0^{\beta}$ and we choose that reference level such that $\sigma \propto D_n^{\delta}$

$$\boxed{\log D_n = 1.3 \log \sigma + C}$$ where C=C(d)

The reference brightness level is 20.75 mag/arcsec^2 in B.

Good for relative distances and usually applied to clusters (e.g. Virgo-Coma)

Secondary Indicators: D_n-σ (~1Gpc)

D_n-σ Relation

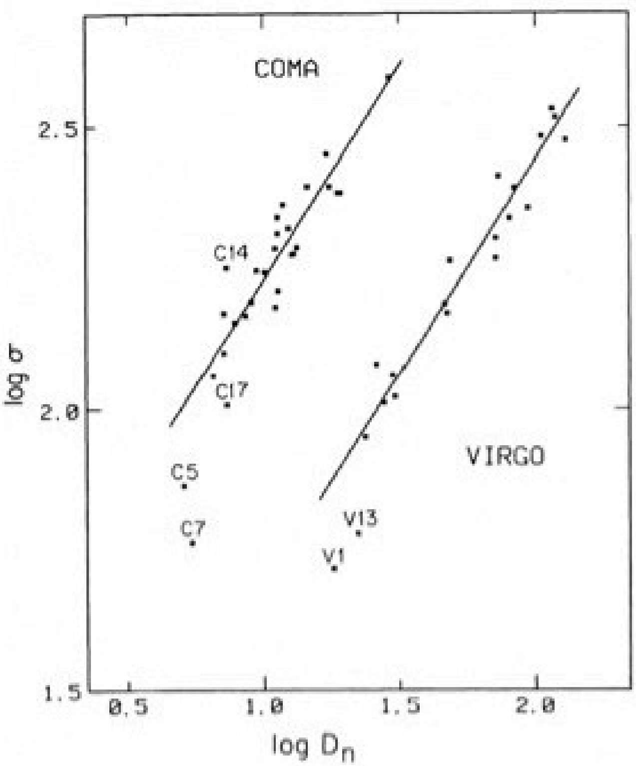

FIG. 1b

FIG. 1.—(*a*) B_T, the total blue magnitude, vs. log σ, the central velocity dispersion, for ellipticals in the Coma and Virgo clusters. These are the variables of the Faber-Jackson relationship. The lines log $\sigma = -0.114B_T + C$, where $C = 3.561$ for Virgo and $C = 3.960$ for Coma, are best median fits, as described in the text. The rms scatters in B_T from these lines are 0.57 mag for Virgo and 0.69 mag for Coma. (*b*) log D_n, the diameter within which the integrated blue surface brightness is 20.75 *B* mag arcsec^{-2}, vs. log σ for the same galaxies. The horizontal scales correspond to a factor of 10 in distance in both figures. The lines log $\sigma = 0.750 \log D_n + C$, where $C = 0.934$ for Virgo and $C = 1.475$ for Coma, are best median fits. The rms scatter in log D_n is 0.059 for Virgo and 0.072 for Coma, a factor of 2 smaller scatter than with the Faber-Jackson relationship.

From Dressler et al (1987) the offset gives the relative Distance, but note the scatter!

Secondary Indicators: Faber-Jackson (~1Gpc)

In the absence of surface-brightness information, still the relationship holds (Faber & Jackson 1976):

$$L \propto \sigma^{\alpha} \text{ with } \alpha \approx 3-4$$

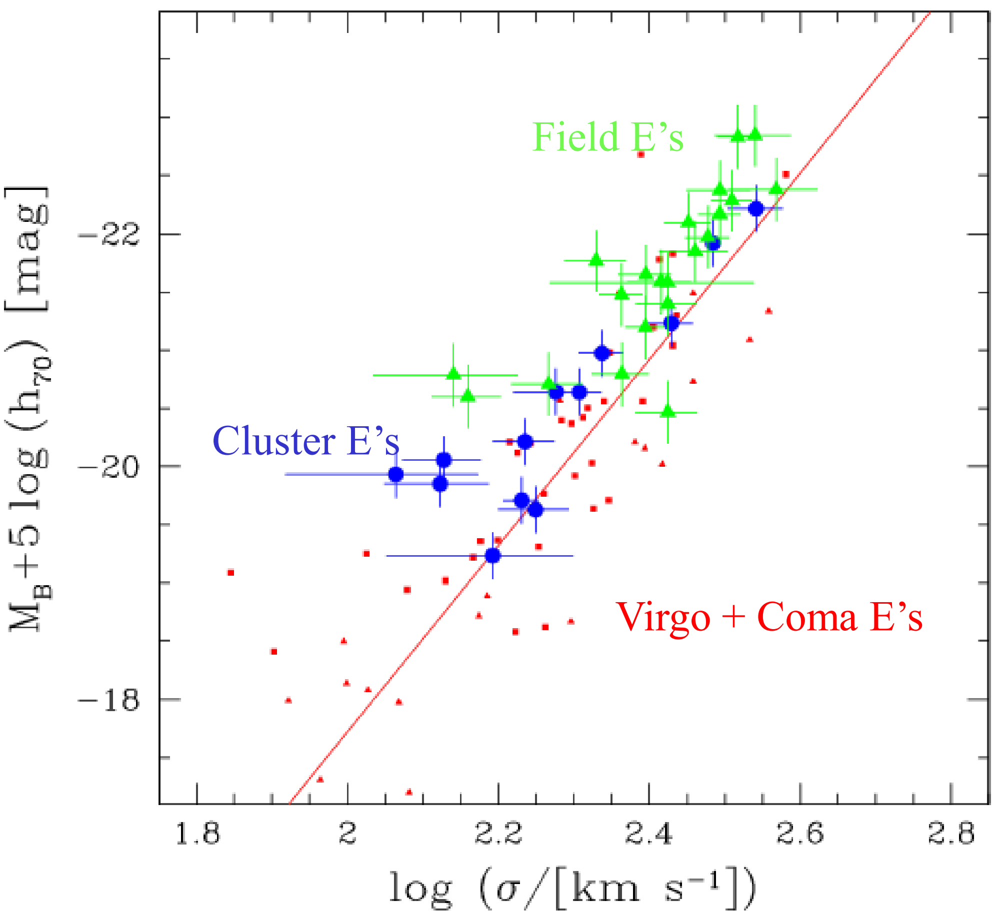

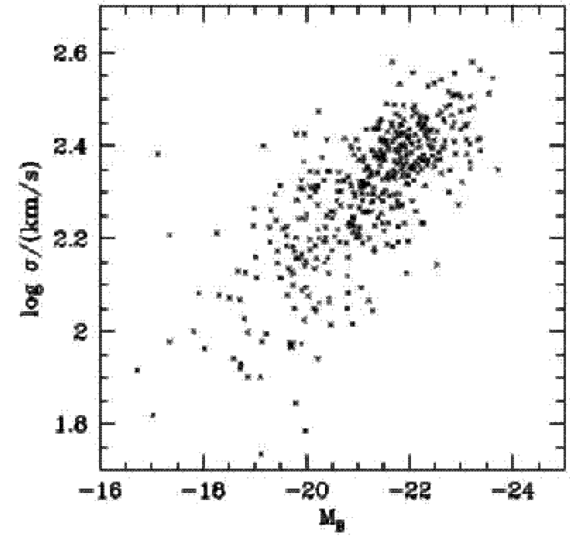

Modest B-evolution of 0.3-0.5mag at z~0.4-0.7

(e.g. Ziegler et al. 2005)

Other Secondary Indicators: Surface Brightness Fluctuations

Statistical fluctuation in the number of stars in a pixel (Tonry & Schneider 1988, Tonry et al. 2000)

A nearby galaxy: 100/pixel ±10% fluctuations
A distant galaxy: 1000/pixel ±3% fluctuations

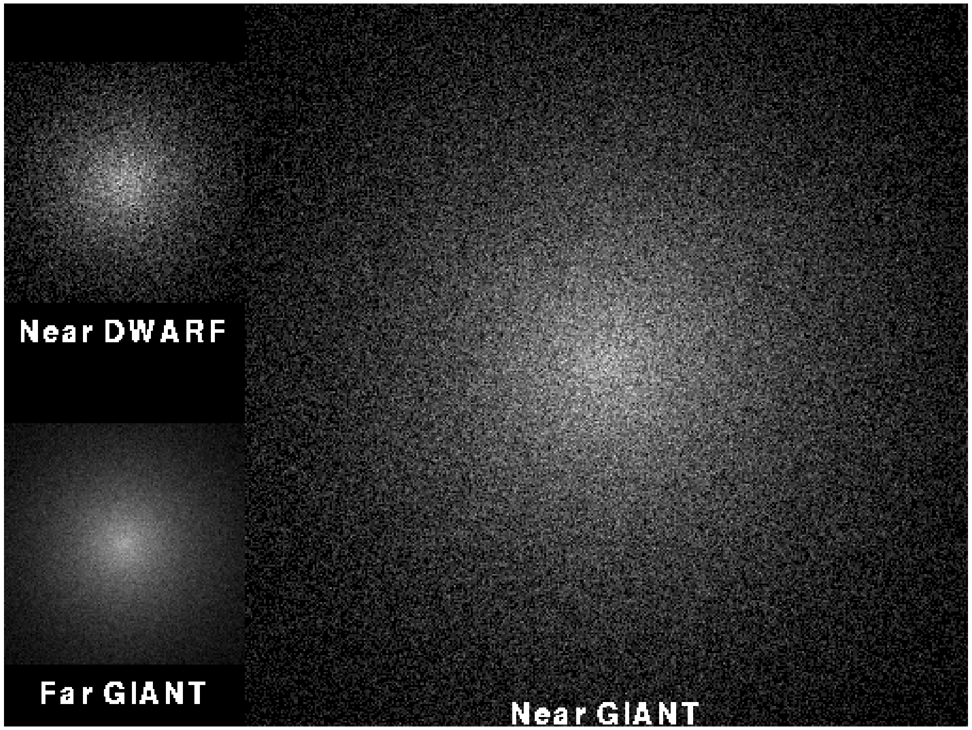

Other Secondary Indicators:

Brightest Galaxy in Cluster

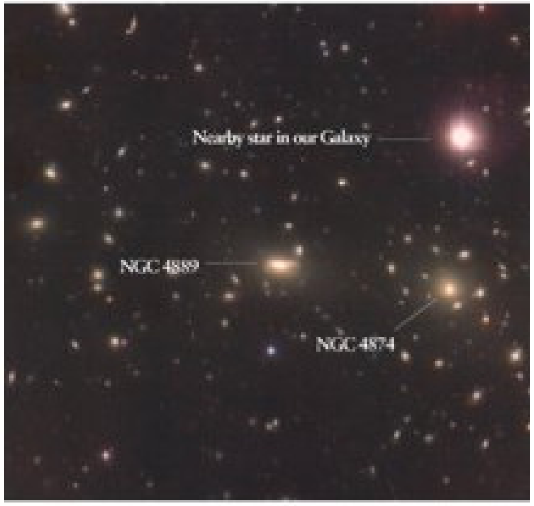

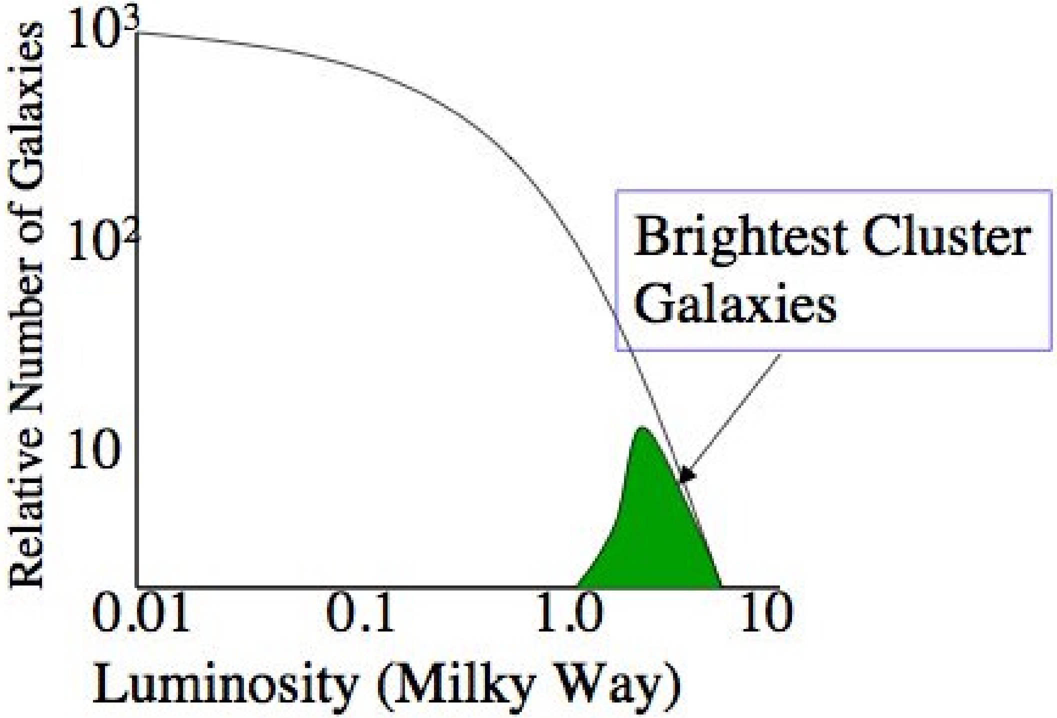

Note the narrow range in luminosity - thus standard candle.

Problem: rich clusters will have bright galaxies, but poor ones probably not

TABLE 1

NUMBERS OF CEPHEID CALIBRATORS FOR SECONDARY METHODS

Secondary Method	σ (%)	N (pre-*HST*)	σ_{mean} (%)	N (post-*HST*)	σ_{mean} (%)
Tully-Fisher relation	± 20[a]	5[b]	± 10	21	± 5
Type Ia supernovae	± 8[c]	0	n/a	6[d]	± 4
Surface brightness fluctuations......	± 9[e]	1	± 9	6	± 4
Fundamental plane....................	± 14	0	n/a	3[f]	± 10
Type II supernovae	± 12[g]	1	± 12	4	± 6

[a] Giovanelli et al. 1997.
[b] M31, M33, NGC 2403, M81, NGC 300; Freedman 1990.
[c] Hamuy et al. 1996.
[d] Using the distances to the host galaxies to SN 1937C, 1972E, 1981B, 1989B, 1990N, and 1998bu, but excluding 1895B, 1960F, 1974G.
[e] Tonry et al. 1997.
[f] Calibration based on Cepheid distances to Leo I group, Virgo and Fornax Clusters.
[g] This paper; Schmidt et al. 1994 distant clusters.

(H_0 Key Project, Freedman et al. 2001)

The value of H_0:

H_0=72±8 km/s/Mpc (Freedman et al. 2001)

(…) . Based on these revised Cepheid distances, we find values (in km s^{-1} Mpc^{-1}) of $H_0 = 71 \pm 2$ (random) ± 6 (systematic) (Type Ia supernovae), $H_0 = 71 \pm 3 \pm 7$ (Tully-Fisher relation), $H_0 = 70 \pm 5 \pm 6$ (surface brightness fluctuations), $H_0 = 72 \pm 9 \pm 7$ (Type II supernovae), and $H_0 = 82 \pm 6 \pm 9$ (fundamental plane). We combine these results for the different methods with three different weighting schemes, and find good agreement and consistency with $H_0 = 72 \pm 8$ km s^{-1} Mpc^{-1} (…)

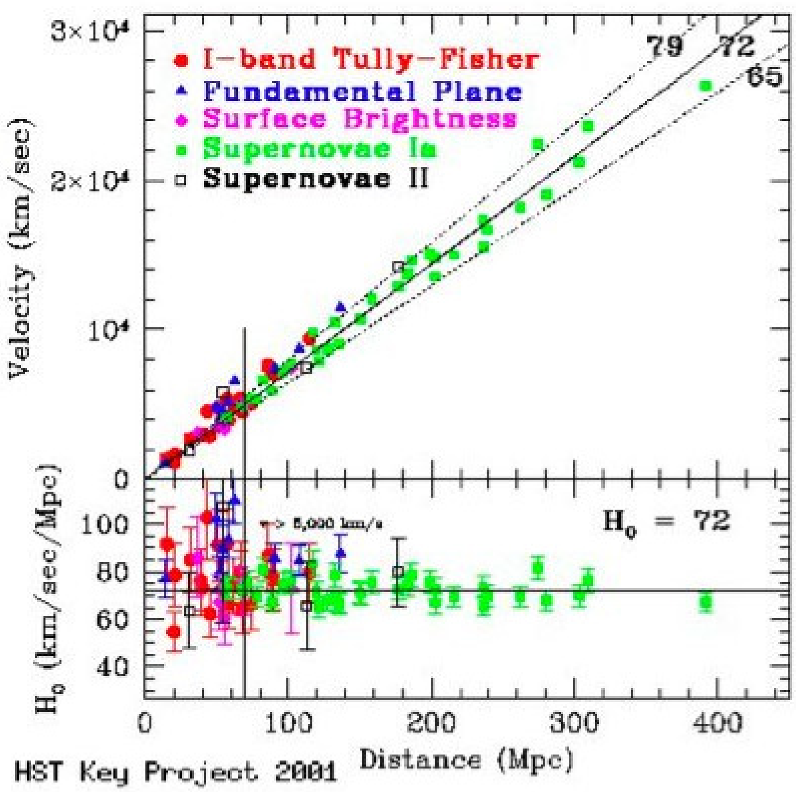

The value of H_0:

H_0=72±8 km/s/Mpc (Freedman et al. 2001)

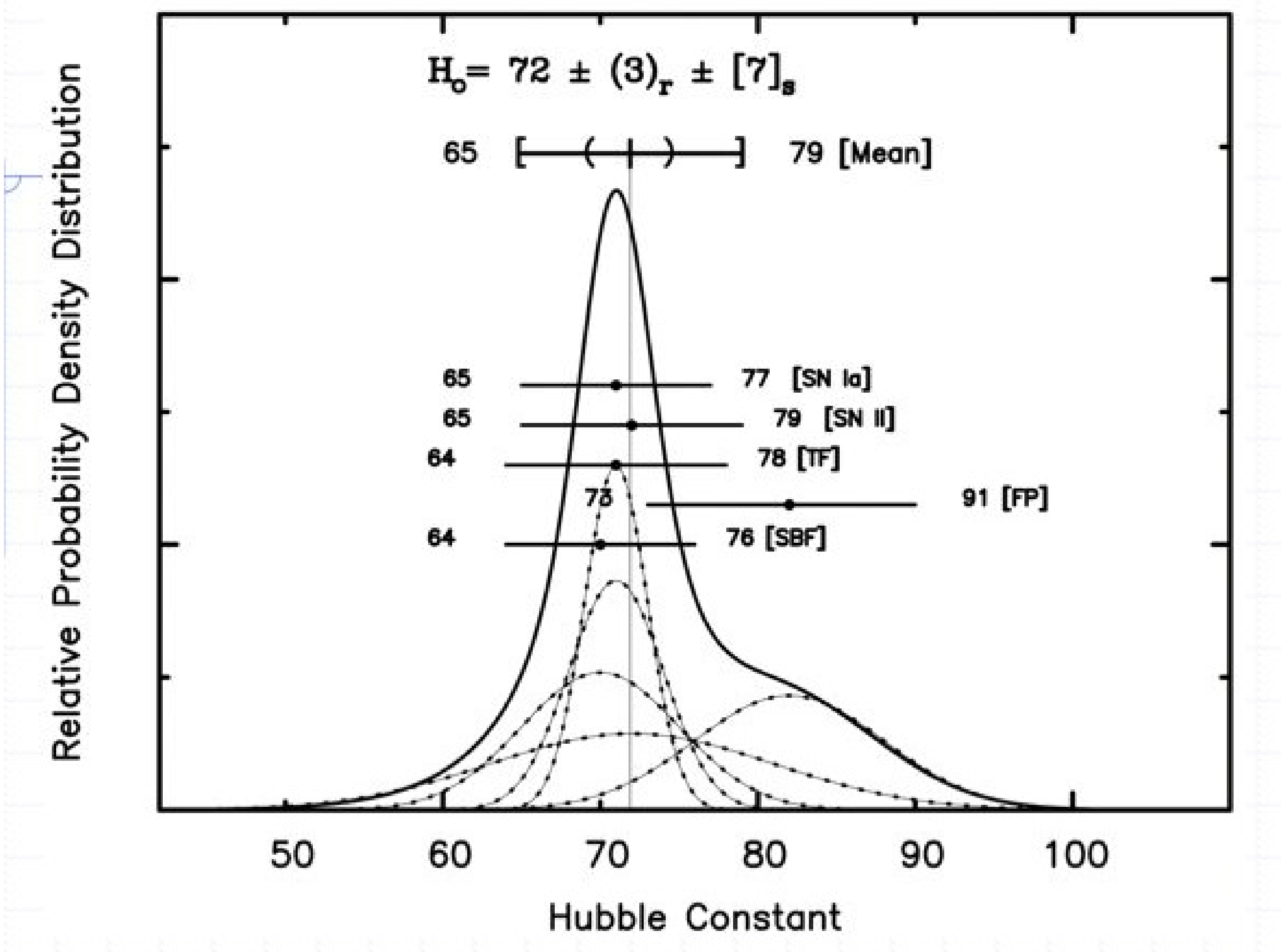

The value of H_0:

H_0=72±8 km/s/Mpc (Freedman et al. 2001)

TABLE 14

OVERALL SYSTEMATIC ERRORS AFFECTING ALL METHODS

Source of Uncertainty	Description	Error (%)
LMC zero point	Error on mean from Cepheids, TRGB, SN 1987A, red clump, eclipsing binaries	±5
WFPC2 zero point	Tie-in to Galactic star clusters	±3.5
Reddening	Limits from NICMOS photometry	±1
Metallicity	Optical, NICMOS, theoretical constraints	±4
Bias in Cepheid PL	Short-end period cutoff	±1
Crowding	Artificial star experiments	+5, −0
Bulk flows on scales >10,000 km s^{-1}	Limits from SN Ia, CMB	±5

NOTE.—Adopted final value of H_0: $H_0 = 72 \pm 3$ (random) $\pm$ 7 (systematic) km s^{-1} Mpc^{-1}.

The value of H_0:

H_0=72±8 km/s/Mpc (Freedman et al. 2001)

TABLE 13

LMC Distance Moduli for Different Methods

Method	$\langle\mu_0\rangle$[a] (mag)	σ (mag)	N	$\langle\mu_0\rangle$[b] (mag)	σ (mag)	N
Cepheids	18.57	±0.14	5	18.52	±0.13	15
Eclipsing variables	18.33	±0.05	3	...	...	...
SN 1987A	18.47	±0.08	4	18.50	±0.12	5
TRGB	18.64	±0.05	2	18.42	±0.15	1
Red clump	18.27	±0.11	10	...	...	...
RR Lyrae variables	18.30	±0.13	7	18.40	±0.19	14
Mira variables	18.54	±0.04	3	18.46	±0.11	4

[a] Based on Gibson 2000 compilation.
[b] Based on Westerlund 1997 compilation.

The value of H_0:

LMC Distance modulus (Gibson 2000)

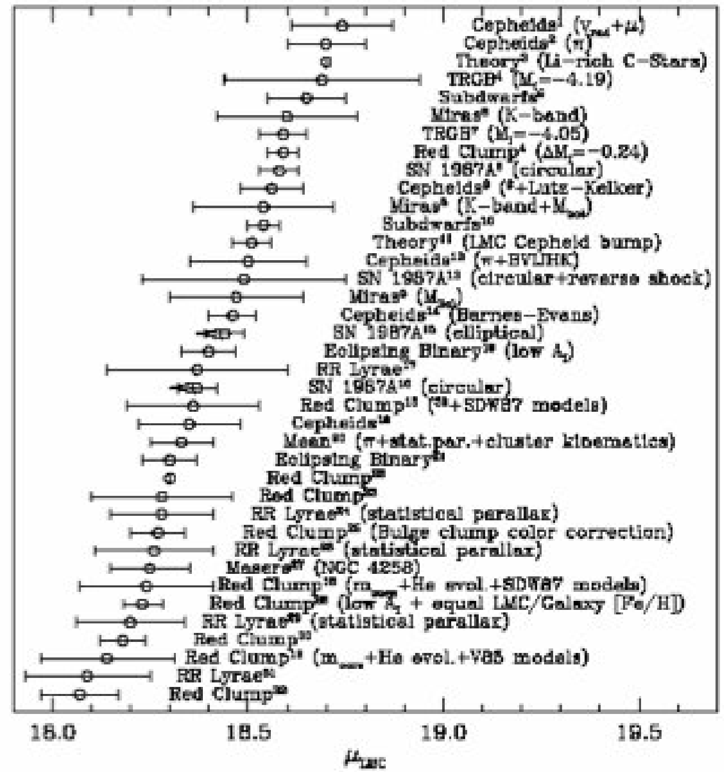

Fig. 1. Compilation of recent distance determinations to the LMC, presented in decreasing order of modulus μ_{LMC}. Cepheids, fitting to local Galactic subdwarf sequences, and theoretical stellar models tend to favor the "long" distance scale (i.e., $\mu_{LMC} \gtrsim 18.5$, while RR Lyrae, red clump luminosities, eclipsing binaries, and masers (indirectly, through NGC 4258) tend to favor the "short" scale (i.e., $\mu_{LMC} \lesssim 18.4$). References: [1]Feast et al. (1998); [2]Feast & Catchpole (1997); [3]Ventura et al. (1999); [4]Romaniello et al. (1999); [5]Reid (1997); [6]van Leeuwen et al. (1998); [7]Sakai et al. (2000); [8]Panagia (1998); [9]Oudmaijer et al. (1998); [10]Carretta et al. (1999); [11]Wood (1998); [12]Madore & Freedman (1998); [13]Garnavich et al. (1999); [14]Gieren et al. (1998); [15]Gould & Uza (1998); [16]Nelson et al. (1999); [17]Luri et al. (1998); [18]Cole (1998); [19]Luri et al. (1999); [20]Popowski & Gould (1999); [21]Guinan et al. (1998); [22]Beaulieu & Sackett (1998); [23]Girardi et al. (1998); [24]Layden et al. (1996); [25]Fernley et al. (1998); [26]Popowski (1999); [27]Maoz et al. (1999); [28]Udalski (1999); [29]Popowski & Gould (1998) and Gould & Popowski (1998); [30]Udalski (1998b); [31]Udalski (1998a); [32]Stanek et al. (1998).

The value of H_0:

LMC Distance modulus (Gibson 2000)
Mean 18.45±0.06
H_0 Key project assumes 18.5
Still the weakest point in the distance ladder

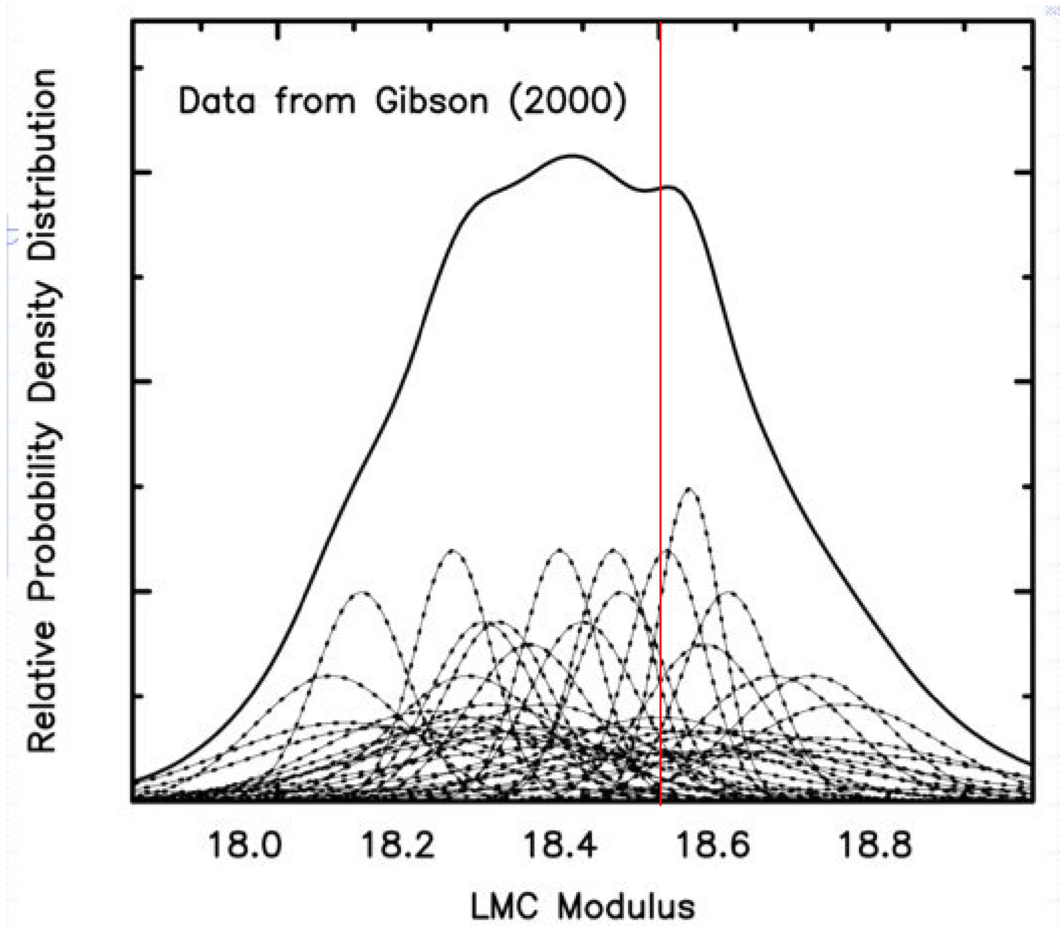

The value of H_0 at 3%: 74.4±3.1 km/s/Mpc

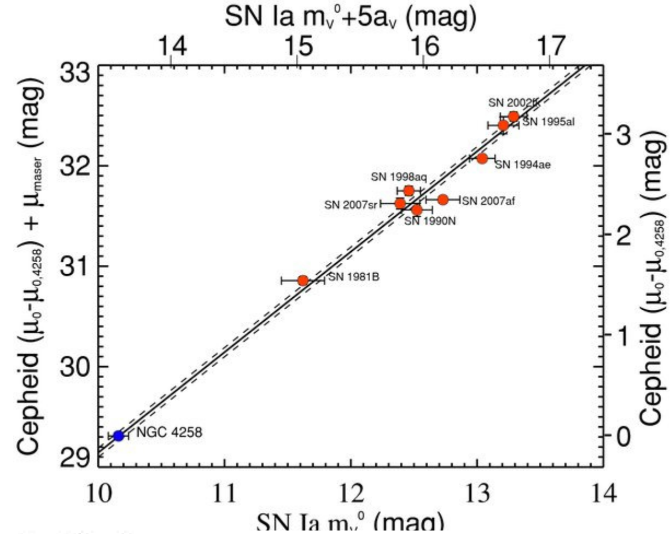

Anchor reference from LMC only to use LMC, MW and NGC4258 (Riess et al. 2011), with homogeneous photometry: simultaneous fit Cepheid and SN relations to find nuisance parameters *zp, b, Z*

$$m_{i,j} = (\mu_{0,i} - \mu_{0,ref}) + zp_{ref} + b \log P_{i,j} + Z\Delta \log[\mathrm{O/H}]$$

$$m^0_{v,i} = (\mu_{0,i} - \mu_{0,ref}) + m^0_{v,ref}$$

H_0 Error Budget for Cepheid and SN Ia Distance Ladders[a]

Term	Description	Previous LMC	R09 N4258	Here N4258	Here All Three[b]
σ_{anchor}	Anchor distance	5%	3%	3%	1.3%
$\sigma_{\mathrm{anchor}-PL}$	Mean of *P–L* in anchor	2.5%	1.5%	1.4%	0.7%[c]
$\sigma_{\mathrm{host}-PL}/\sqrt{n}$	Mean of *P–L* values in SN hosts	1.5%	1.5%	0.6 %	0.6%
$\sigma_{\mathrm{SN}}/\sqrt{n}$	Mean of SN Ia calibrators	2.5%	2.5%	1.9%	1.9%
σ_{m-z}	SN Ia *m–z* relation	1%	0.5%	0.5%	0.5%
$R\sigma_{\lambda,1,2}$	Cepheid reddening, zero points, anchor-to-hosts	4.5%	0.3%	0.0%	1.4%
σ_Z	Cepheid metallicity, anchor-to-hosts	3%	1.1%	0.6 %	1.0%
σ_{PL}	*P–L* slope, $\Delta\log P$, anchor-to-hosts	4%	0.5%	0.4%	0.6%
σ_{WFPC2}	WFPC2 CTE, long-short	3%	0%	0%	0%
Subtotal, σ_{H_0}		10%	4.7 %	4.0%	2.9%
Analysis systematics		NA	1.3%	1.0%	1.0%
Total, σ_{H_0}		10%	4.8 %	4.1%	3.1%

The value of H_0:

Publications of the Astronomical Society of the Pacific
108: 1073–1082, 1996 December

H_0: The Incredible Shrinking Constant 1925–1975

VIRGINIA TRIMBLE

Physics Department, University of California, Irvine, California 92717 and Astronomy Department, University of Maryland, College Park, Maryland 20742

Received 1996 September 13; accepted 1996 September 30

ABSTRACT. The story of the Hubble constant logically begins just where the Curtis–Shapley debate on the distance scale of the universe ended, with Hubble's discovery of Cepheid variables in several nebulae that we now recognized as galaxies within the Local Group, which settled the issue of the existence of external galaxies. Hubble's own value of H was in the range of 500–550 km s^{-1} Mpc^{-1}. The "best buy" value shrank in several large steps beginning in 1952, each being predicated on the recognition of some fundamental mistake in the previous distance scale calibrations. But it shrank more for some workers than for others, and by 1975 there was a clear polarization between a "long" and a "short" distance scale. On the theoretical side, important events were the recognition that general relativity permits, indeed nearly requires, an expanding universe; the gradual elimination of alternative explanations of redshift–distance relations; and the repelling of a late assault in the form of steady-state cosmology, within whose framework H_0 is a well-defined, never-varying number of only moderate importance.

The value of H_0:

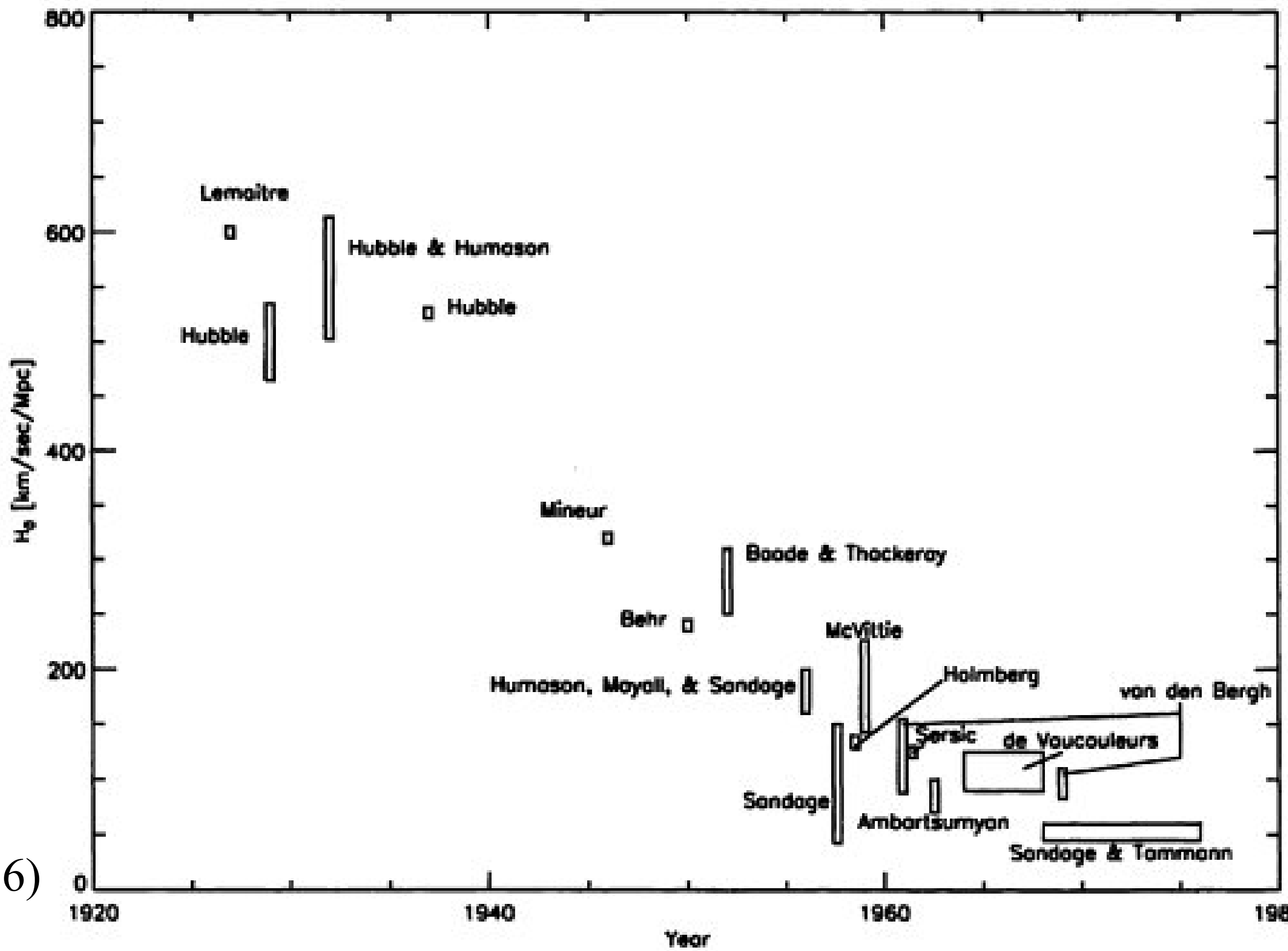

(Trimble 1996)

FIG. 1—Published values of the Hubble constant from Lemaître (1927) to the hardening of the battle lines. Rectangle dimensions are intended to suggest a range of values/uncertainties or a range of dates. Except where the errors listed below are larger, all uncertainties were claimed to be of order 10% or less (occasionally much less). A straight-line fit to the numbers from 1927 to 1965 or so would have suggested that the Hubble constant might have become negative within a decade or two (discovered by astronomy graduate students at Caltech in the 1960s and undoubtedly by many others). This did not actually happen. The numerical values represented are Lemaître 600, Hubble 465, 513, 535; Hubble and Humason 526; Mineur 320; Behr 240; Baade and Thackeray 280±30; Hubble, Mayall, and Sandage 180±20; Sandage 75 (+75,−40); Holmberg 134±6; McVittie 143–227; Sersic 125±5; van den Bergh 100 (+20, −12), 120 (+25,−20); Ambartsumyan 70–100; de Vaucouleurs 125, 100±10, 100±10; van den Bergh 95 (+15,−12); Sandage and Tammann 45–60.

H0 without the distance ladder:

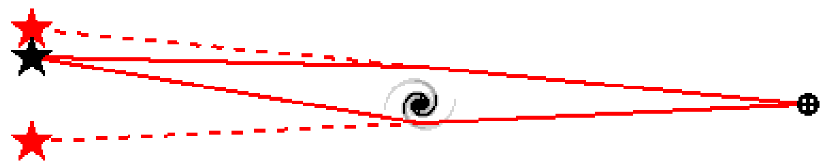

- Gravitational lens time delays
  - Assuming the mass model for the lensing galaxiy of a gravitationally lensed quasar is well-known (!?!), the different light paths taken by various images of the quasar will lead to time delays in the arrival time of the light to us. This be can be traced by the quasar variability.
  - This has been done for a handful of objects, find values of H0 between 50 and 70 km/s/Mpc ... lower on average than the Key Project values. (e.g. 0957+561 Kundic et al. 1997)
  - If the lensing galaxy is in a cluster, we also need to know the mass distribution of the cluster and any other mass distribution along the line of sight. The modeling is complex!
  - Because of this, gravitational lens time delay measurements depend on Ω_Λ and Ω_M.

H0 without the distance ladder:

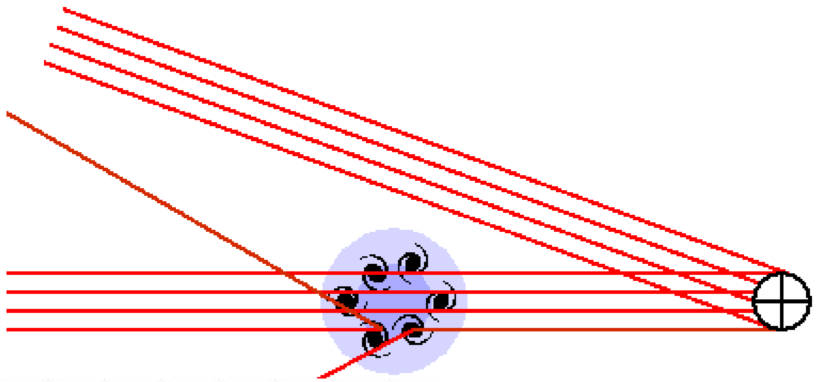

- **The Sunyaev-Zel'dovich Effect**
  - The electrons in the intracluster medium will scatter the background photons from the cosmic microwave background (CMB) to higher energies (frequencies) and distort the blackbody spectrum
  - If we can measure the electron density and temperature of the ICM along the line of sight from x-ray measurements and we assume the cluster is spherical (??) we can determine the distance to the cluster from the shift in the CMB spectrum
  - Published values for H_0 range from 40 – 80 km/s/Mpc, most recent is H_0 = 60 +/- 10 km/s, but there are large systematic uncertainties (e.g. 38 clusters Bonamonte et al. 2006)
  - Potential uncertainties include cluster substructure or shape (prolate instead of spherical). It's non-trivial to measure the x-ray temperature to derive the density at high redshifts.
  - Need larger surveys for S-Z clusters at higher redshifts, these are underway!

H0 without the distance ladder

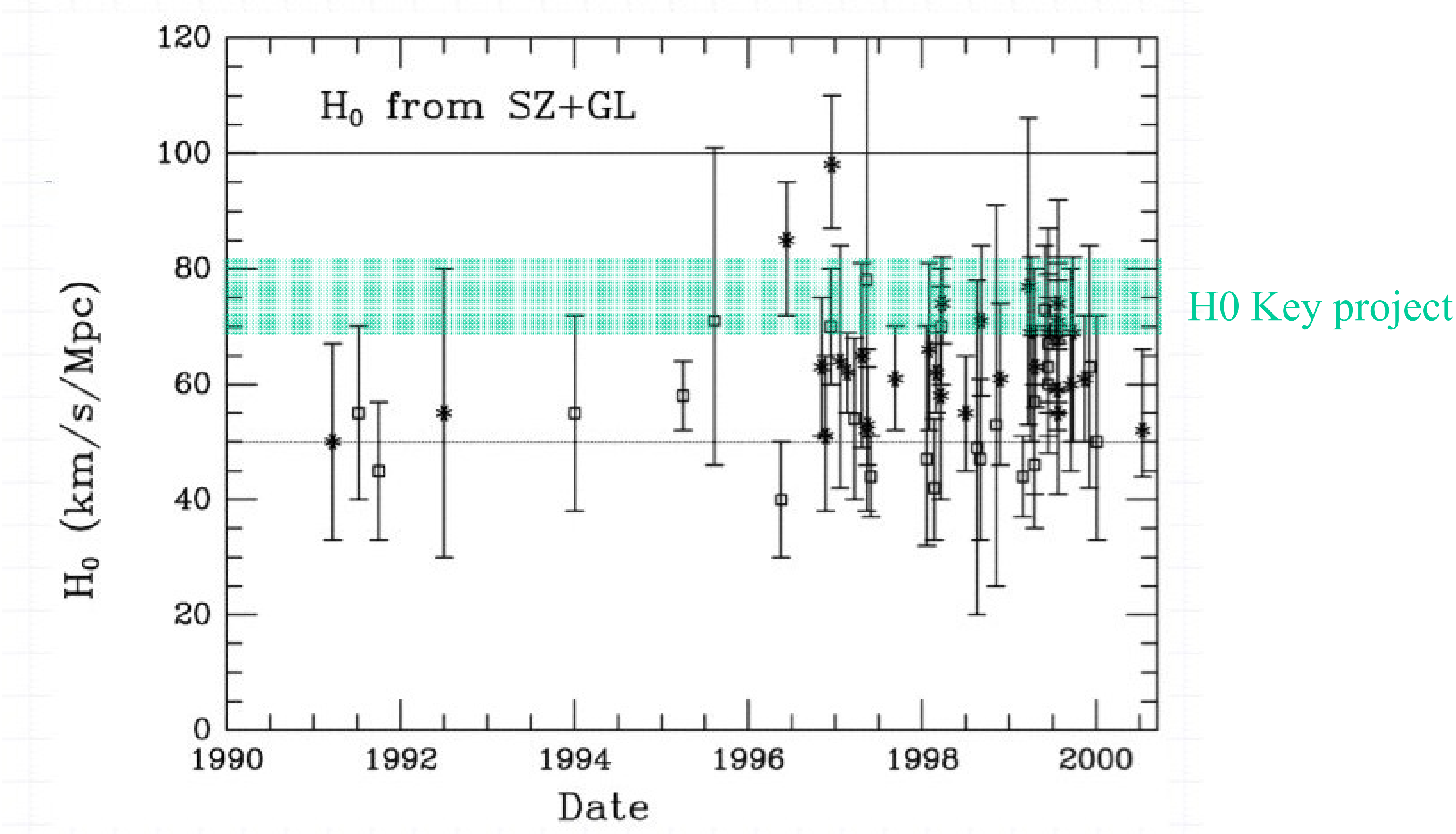

The original Hubble diagram

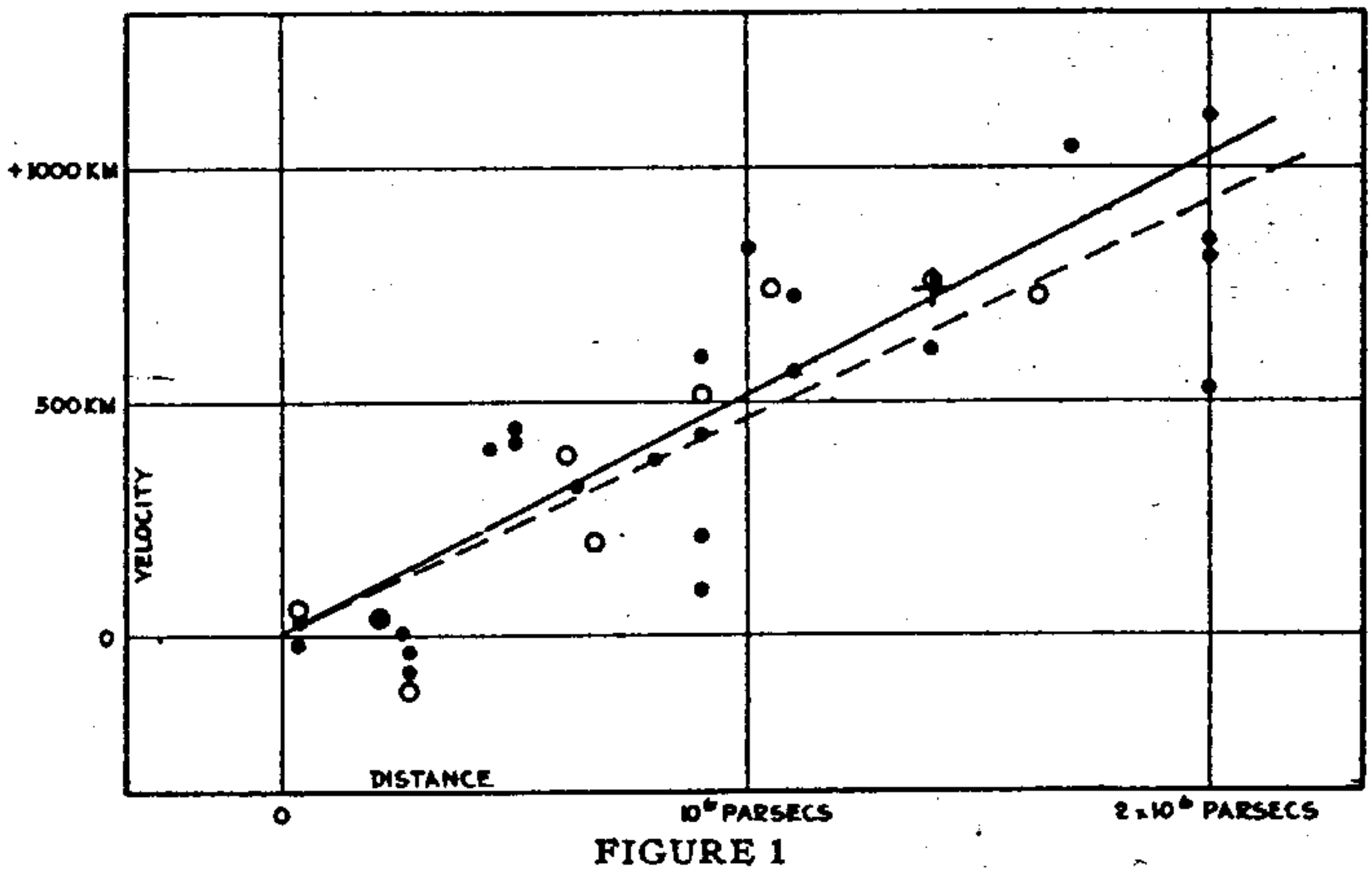

Hubble (1936)